Marked-up copy

Application of an Energy Based Security Method to Voltage Instability in Electrical Power Systems

By

Thomas J. Overbye

Preliminary Report

Supervised by Professor Christopher L. DeMarco

Department of Electrical and Computer Engineering

College of Engineering

University of Wisconsin-Madison

Madison, Wisconsin 53706

January, 1990

Contents

Chapter 1 - Introduction

1.1 Voltage Instability in Power Systems

The availability of reliable and economical electrical power is vitally important to the well being of our economy. Over the last few decades electrical systems throughout the industrialized world have changed from relatively localized systems to large interconnected systems with tens or hundreds of millions of customers who often receive power from generators hundreds or even thousands of miles distant. This high degree of interconnection makes it essential that the high voltage transmission system be operated in both a secure and economical manner. A secure operating point is one where the system can adequately supply the necessary power to all customers even in the event of statistically likely contingencies (such as transmission line outages or loss of generators). The system security requirement, however, is often contradictory to economically optimal operation, which can require operation of the system near its limit in order to take advantage of distant, low cost generation.

Traditionally the balancing of system security with economical operation has presented utility operators and planners with the two problems of thermal loading and angular (or transient) stability. The former problem requires that the current on each individual transmission line or transformer be less than a limit derived from the thermal characteristics of the device and occasionally the ambient conditions. The latter problem requires that the system be able to return to a secure operating following a large scale disturbance (e.g. loss of a generator). Many techniques, such as optimal powerflows, have been developed to deal with these problems. However over the last few years, as the operating conditions for large power systems have evolved, a new problem has been developing which is often referred to as voltage instability or voltage collapse.

Voltage instability is a phenomenon characterized by the voltages throughout a large portion of the high voltage transmission system gradually declining over a period of minutes to hours. Eventually, if system loading continues to increase, the voltages suddenly collapse, resulting in either local or system-wide blackouts. To illustrate the basic mechanics of voltage collapse, consider the system shown in Figure 1-1. The region on the left represents an area of the power system with excess generation capacity, while the region on the right is characterized by high demand (load). Power is therefore transferred through the transmission lines connecting the regions. This system is a rough equivalent to many large

power systems, which depend upon distant generation to serve large urban loads. Figure 1-2 shows the approximate voltage in the load area as a function of the amount of power interchanged between the two areas. For low levels of interchange the sensitivity of the voltage to amount of power interchanged is rather low, resulting in little drop in voltage at the load end. However as the interchange is increased, the voltage sensitivity also increases, first gradually, but then with increasing rapidity. The net effect is an increasingly rapid drop in voltage. Eventually a critical power level is reached, characterized by an infinite voltage sensitivity. An attempt to transfer more than this critical amount of power results in loss of a stable operating point, and eventual voltage collapse.

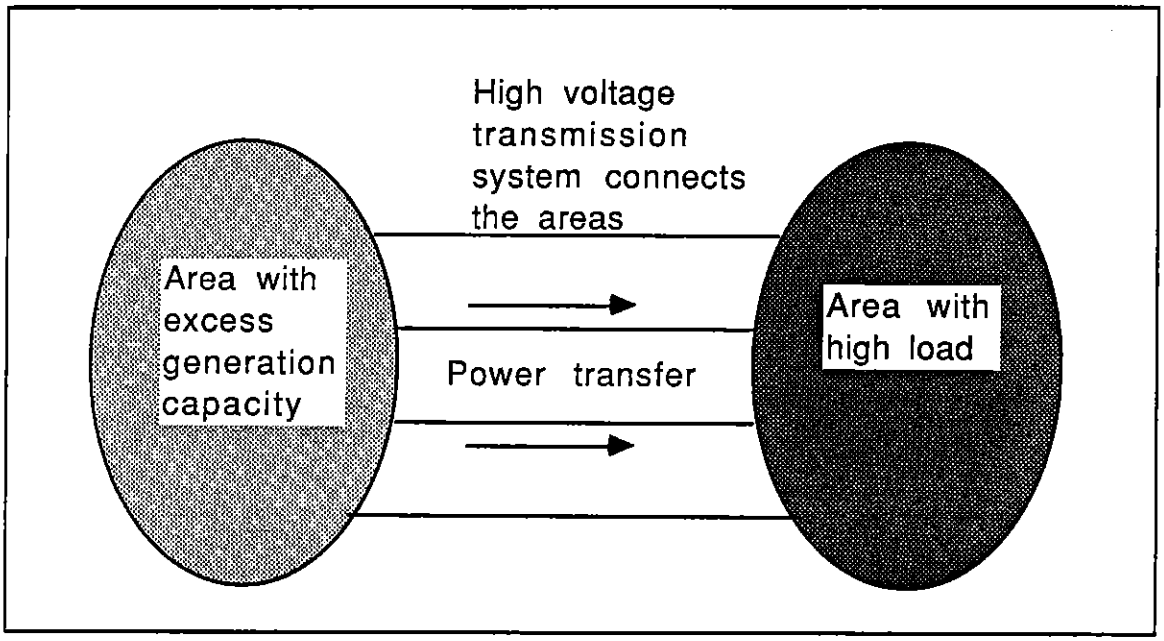

Figure 1-1 : Electric Power System Simplification

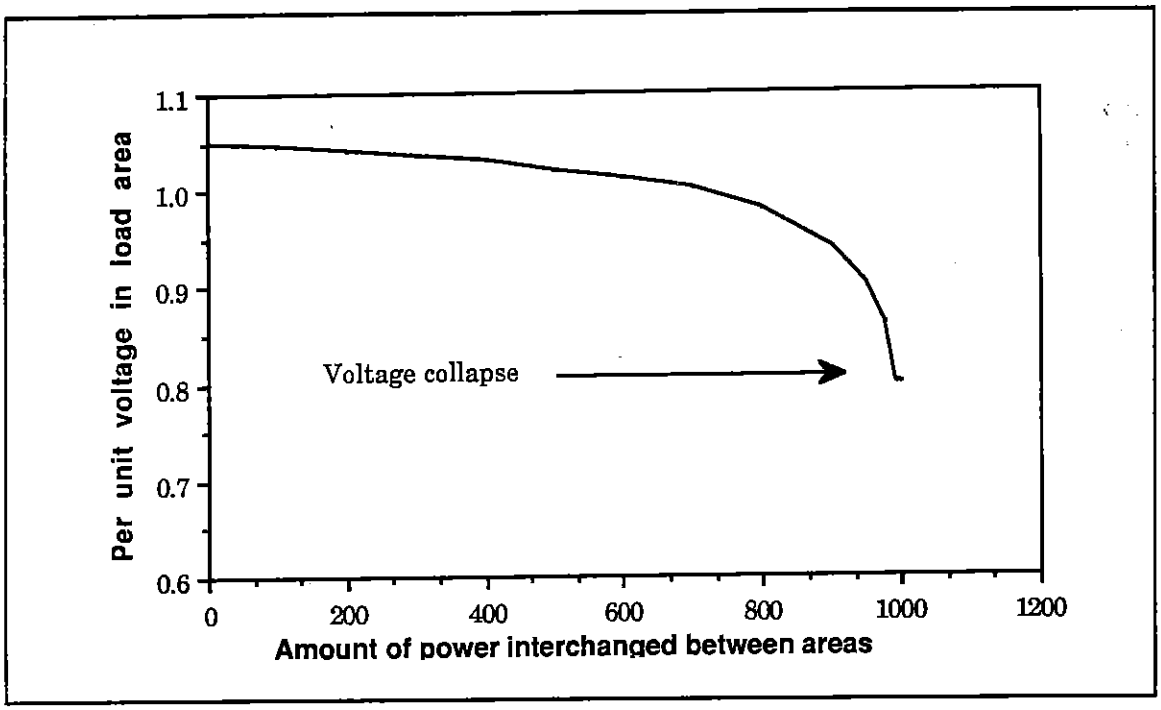

Figure 1-2 : Load Area Voltage as a Function of Power Transfer

A large scale voltage collapse induced blackout occurred in 1978 in France [1]. Over the course of 26 minutes, voltages throughout the entire French high voltage transmission system gradually declined from normal voltage of approximately 410KV to less than 340KV. The cause of this collapse was large power transfers between the French system and other European electric systems. A more recent incident occurred in Tokyo during the summer of 1987 [2]. There, high load demand and the necessity of importing power from distant generators caused a power outage of 8000 MW, affecting about 2.6 million people. The time period of this collapse was about 20 minutes, again with the voltages gradually declining throughout a large portion of the Tokyo system. Domestically, near-record loads and high power transfers during 1987 caused voltages in the high voltage transmission system in Illinois and Indiana to decline by as much as 12% over the course of hours [3]. Voltage security problems in this time frame have also occurred in the Northeastern U.S., with at least 8 incidents documented in 1988 [4].

Presently utilities assess the security of their systems on-line via security-constrained optimal powerflow (OPF) programs [5] (by on-line we mean that the present state of the power system is being analyzed, with results of the analysis available within seconds to minutes). These programs try to optimize the system by recommending various controller moves (such as changes in generator MW outputs, transformer tap positions, etc.) to

minimize system operating cost while insuring that there are no security violations. Examples of security violations would include transmission line flows above some thermal limit, or bus voltage magnitudes below some limit. Typically limits are determined a priori off-line. While this approach has proved useful in dealing with problems of a thermal overload nature, it is inadequate for a number of reasons in predicting the onset of voltage instability. First, voltage instability problems have been shown to occur in systems where voltage magnitudes never decline below levels that have traditionally been deemed acceptable in off-line planning studies [6]. Thus since voltages never decline below their limits (until the system totally collapses), they never become active constraints in the OPF problem. Therefore no control action is initiated. Second, near the point of collapse, voltage variations can be extremely sensitive to changes in load and other system parameters [7]. Knowledge of the voltage level only at the current operating point may not be sufficient since a small change in the system operating point could cause a large voltage drop. Lastly, in order to avoid the high cost of constructing new lines, utilities would like to operate their systems in such a manner as to maximize the capacity from their existing transmission system. However to do this they need an indication of how close they are to the point of voltage collapse. Current OPF programs provide no such proximity indicator.

The absence of an easily computable proximity indicator to voltage collapse has meant that utilities must calculate system limits (such as maximum MW transfer) off-line using powerflow programs. In [8] it is reported that engineers must run hundreds of powerflow simulations daily using assumed future operating conditions in order to predict what these limits should be. An obvious difficulty of such an off-line approach lies in predicting the future conditions. Worst case scenarios are often assumed. This can result in either overly conservative limits, which prevent the utilities from taking advantage of more economical but more distant generation, or blackouts when the actual conditions are different from the assumed conditions. The magnitude of this problem can be seen in [8] where one of the larger utilities in the US reported that during 1987 they were not able to utilize their available generators as economically as possible 74% of the time, and that in approximately 96% of these instances the problem was due to reactive (voltage) limitations in the transmission system. Clearly a new approach to this problem is needed.

The goal of this thesis proposal is to develop a method based upon energy function techniques which can accurately determine how close a power system is to the point of voltage instability. The computational requirements of this method should be such that it can effectively be used on-line to analyze a reasonably sized system.

1.2 Power system Stability

In order to motivate the use of energy function methods, the concept of power system stability is briefly reviewed. Power systems are nonlinear, often slowly varying systems which are subject to a number of disturbances. Such a system can be represented by the following set of time-varying differential and algebraic equations:

$$\begin{aligned} \dot{\mathbf{x}} &= \mathbf{f}(\mathbf{x}(t), \mathbf{y}(t), \mathbf{u}(t)) \\ \mathbf{0} &= \mathbf{g}(\mathbf{x}(t), \mathbf{y}(t), \mathbf{u}(t)) \end{aligned} \tag{1-1}$$

where

- $\mathbf{x}$ - state variables (e.g. bus voltage phase angles)
- $\mathbf{y}$ - algebraic variables (e.g. bus voltage magnitudes)
- $\mathbf{u}$ - input variables (which includes the changing load/generation injections and other disturbances)

A system of the form described by (1-1) is said to have an equilibrium point $\mathbf{x}_0$ at time $t_0 \in R_+$ if for a fixed known input, $\mathbf{u}(\bullet)$, $\mathbf{f}(\mathbf{x}(t), \mathbf{y}(t), \mathbf{u}(t)) = 0$, $\forall\ t \geq t_0$. Thus the mathematical definition requires that once the system reaches its equilibrium point $\mathbf{x}_0$ at time t_0 it remains there ad infinitum. However for realistic power systems this is never the case. The system state variables are subject to constant variation in response to both sporadic large disturbances to the system (e.g. loss of a large generator) along with the time variation in the loads of individual customers. However, this load variation is normally of the form of a slowly varying average value (normally with its largest component having a 24 hour period) along with a small (a few percent) random variation about this average value. Research into aggregate load models has suggested that such small random effects may be modeled by a white or colored noise term in the load [9]. Ignoring for the moment the infrequent large disturbances, we can express $\mathbf{u}(t)$ as

$$\mathbf{u}(t) = \mathbf{u}^{slow}(t) + \mathbf{u}^{small}(t)$$

where

$\mathbf{u}^{slow}$ - slowly varying average load component

$\mathbf{u}^{small}$ - zero mean, "small" magnitude load variation

If the time scale of the problem of interest is sufficiently short, relative to the variation in $\mathbf{u}^{slow}(t)$, stability studies often make the assumption that

$$\mathbf{u}^{slow}(t) = \hat{\mathbf{u}} \text{ (constant)}$$
$$\mathbf{u}^{small}(t) = 0$$

and can therefore rewrite (1-1) as

$$\begin{aligned} \dot{\mathbf{x}} &= \mathbf{f}(\mathbf{x}(t), \mathbf{y}(t), \hat{\mathbf{u}}) = \hat{\mathbf{f}}(\hat{\mathbf{x}}, \hat{\mathbf{y}}) \\ \mathbf{0} &= \mathbf{g}(\mathbf{x}(t), \mathbf{y}(t), \hat{\mathbf{u}}) = \hat{\mathbf{g}}(\hat{\mathbf{x}}, \hat{\mathbf{y}}) \end{aligned} \qquad (1\text{-}2)$$

Since $\hat{\mathbf{u}}$ is now a constant, (1-2) is an autonomous system. Therefore if $[\hat{\mathbf{x}}_o, \hat{\mathbf{y}}_o]$ is an equilibrium point of (1-2) at some time t_o, we know that it is an equilibrium point at all time thereafter. Then if the true system has a solution $[\mathbf{x}(\bullet), \mathbf{y}(\bullet)]$ for some given $\mathbf{u}(\bullet)$, we would expect that for a given time $\hat{t}$ with an instantaneous input of $\mathbf{u}(\hat{t}) = \hat{\mathbf{u}}$, $\mathbf{x}(\hat{t})$ and $\mathbf{y}(\hat{t})$ from (1-1) should be "close" to $\hat{\mathbf{x}}(\hat{t})$ and $\hat{\mathbf{y}}(\hat{t})$ from (1-2). One approximates the actual time varying input $\mathbf{u}(\bullet)$ with a time invariant input by "freezing" $\mathbf{u}$ at a given time $\hat{t}$. We can then define a "frozen equilibrium" of (1-1) as $[\hat{\mathbf{x}}_o, \hat{\mathbf{y}}_o]$, and then determine the stability of the autonomous system relative to this equilibrium point. The approximation of the actual time varying system by a time invariant system is often the "hidden assumption" in most power system stability analysis. The validity of this assumption is dependent upon how fast the system inputs are changing relative to the dynamics of the system and the time scale of the problem.

If the time variation in $\mathbf{u}^{slow}$ is truly "slow enough", relative to the dynamics of the system, and in the absence of any disturbances ($\mathbf{u}^{small} = 0$), the system state would sit in a negligibly small neighborhood of the frozen equilibrium point. This point would gradually change on the time scale of $\mathbf{u}^{slow}$, and if the system is asymptotically stable, the state would track this slow variation. As noted above, this is never precisely the case for an actual system since the state is constantly being perturbed away from this equilibrium point by various system disturbances. In addition to the time scale classification described

above, one can also classify disturbances as either small disturbances (modeled by $\mathbf{u}^{small} \neq 0$) or large disturbances. By definition, a small disturbance is an event for which the system state remains in the neighborhood of the frozen equilibrium point and for which linearized models are accurate. These small magnitude random load variations add a small amount of "energy" to the system and thus are constantly perturbing the state away from its equilibrium point. This energy is normally dissipated through damping in the system. The classification of system stability related to small scale disturbances is known as steady-state stability. Steady-state stability is typically determined by linearizing the system about the equilibrium point of interest and then requiring that all eigenvalues have strictly negative real parts. For an actual system at its normal operating range, this is a minimal requirement. Once this eigenvalue requirement is satisfied, the effects of these small random variations are usually considered negligible and are typically ignored in normal power system analysis.

The large scale disturbances are events which suddenly drive the state far away from its equilibrium point, and/or change the equilibrium by changing the system structure. Examples of large scale disturbances are loss of generators, loss of a transmission line, or a fault on the system. Following such an event the question to be answered is whether the system will return to a frozen equilibrium point (which may be different from the pre-disturbance equilibrium point). This classification of stability is known as transient stability. For $t < t^d$ (time when disturbance is applied to the system) the system equations are assumed to be the following:

$$\begin{aligned} \dot{\mathbf{x}} &= \mathbf{f}(\mathbf{x}(t), \mathbf{y}(t), \hat{\mathbf{u}}) &= \mathbf{0} \\ \mathbf{0} &= \mathbf{g}(\mathbf{x}(t), \mathbf{y}(t), \hat{\mathbf{u}}) \end{aligned}$$

where $\hat{\mathbf{u}}$ is a constant and the system is assumed to have reached its frozen equilibrium. At $t = t^d$ the disturbance is applied to the system, possibly changing $\hat{\mathbf{u}}$, $\mathbf{f}(\bullet)$, and $\mathbf{g}(\bullet)$. For $t \geq t^d$ the new equations are

$$\begin{aligned} \dot{\mathbf{x}} &= \mathbf{f}^d(\mathbf{x}(t), \mathbf{y}(t), \mathbf{u}^d) \\ \mathbf{0} &= \mathbf{g}^d(\mathbf{x}(t), \mathbf{y}(t), \mathbf{u}^d) \end{aligned}$$

Note that in the general case a number of individual disturbances could be applied to the system at separate discrete times (to model, for example, the action of line reclosers or protective relays). However since $\mathbf{u}^d$ is modeled as a constant during the time period

between disturbances, the system can be considered time invariant during this time segment. This assumption that $\mathbf{u}^{slow}(t)$ = constant and $\mathbf{u}^{small}(t) = 0$ is typically valid since the time frame during which the system either reaches a stable equilibrium point, or loses synchronism (unstable) is seldom more than a few seconds. Thus the ultimate determination of whether a system has transient stability is a function of the pre-disturbance operating point and which large disturbances we choose to apply to the system. From a more formal mathematical viewpoint, steady state stability implies the equilibrium of interest is asymptotically stable. A transiently stable system and disturbance implies that the initial state "resulting" from the disturbance is inside the post-disturbance equilibrium's region of attraction. Clearly any system can be considered to be transiently unstable if the disturbance is large enough (consider the disturbance defined to be the loss of all generation in the system). Normally a system is called transiently stable if it can return to a stable equilibrium point following any credible disturbance. However the key point is that, except for a small number of discrete time disturbances, a time invariant $\mathbf{u}$ is assumed throughout the problem.

Returning again to the problem of voltage instability, we first note that most reports of voltage collapse seem to indicate that it was not directly caused by a large disturbance in the system. This is one of the features that distinguishes voltage collapse from transient stability. Instead the system operating point is moving (on a time scale of minutes to hours), usually with gradually increasing loads, from a state of relative security to one of vulnerability. Since voltage instability is driven by the time variation in $\mathbf{u}(t)$, clearly the earlier assumption of a time invariant system is no longer possible. However this future variation in $\mathbf{u}(t)$ is known only approximately at best. Additionally, as the system state evolves in response to $\mathbf{u}(t)$, various automatic control system (e.g. LTC transformers and generator reactive power outputs) will act upon the system, trying to hold the various state values close to their setpoints. Thus the determination of a system's voltage stability involves prediction of behavior in a nonlinear, time varying system whose input function is only approximately known.

1.3 Review of Work by Others in Voltage Collapse

As was mentioned earlier, utilities are continually confronted with the problem of how to operate their systems in both a secure and economical manner. In order to solve this problem, the typical utility must determine the settings of a few hundred controllers (e.g.

MW output of a generator, MW transactions with other utilities, voltage setpoint of a generator, transformer tap position, etc.) in order to supply power to about 1000 time varying aggregate loads (with each load normally representing hundreds or thousands of customers) so that economy is maximized and security is maintained. In order to assess system security, it is necessary that the utility have some measure to determine how close the system is to voltage collapse. In this section the various methods appearing in the literature and in standard industry practice of assessing this voltage security are reviewed.

Intuitively, the problem of determining proximity to voltage collapse can best be explained by reference to Figure 1-3. The current stable, frozen equilibrium of the power system can be thought of as being located at point **p** within a region called the feasible space. Each point in the feasible space corresponds to a separate stable operating point, which corresponds to some value of the input **u**. Note that the dimensionality of this space is the same as the dimensionality of **u**. As $\mathbf{u}^{slow}$ varies with time (both through customers changing their loads and through actions of the controllers mentioned in the previous paragraph), the location of **p** also varies. Surrounding the feasible space is the infeasible space, which is defined as those values of **u** which do not possess a stable operating point. If we assume that $\mathbf{u}^{small} = 0$ and that the variation in $\mathbf{u}^{slow}$ is very much slower than the dynamics of the system, then the boundary between these two regions is quite distinct. This is never completely true in practice and therefore we have some points, in the feasible region close to the boundary, which although they possess steady-state stability, their "energy wells" are shallow enough that even the small energy they receive from $\mathbf{u}^{small}$ is enough to drive them away from their equilibrium points. However, the assumption we use for power systems is that the width of the "band" about the boundary containing these marginally stable points is small compared to the variation in **p** caused by $\mathbf{u}^{slow}$.

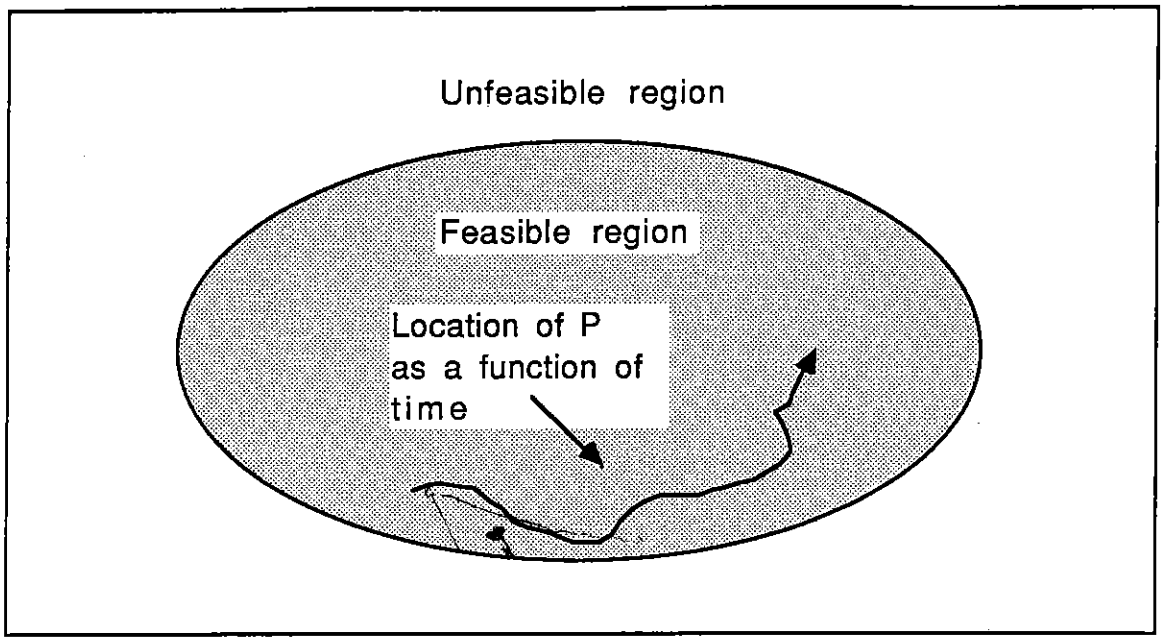

Figure 1-3 : Time Variation in Power System Operating Point

Determining the voltage security of any operating point **p** can then be stated succinctly as simply determining how close **p** is to the feasibility boundary. Two problems arise however. First, computing the feasibility boundary is computationally prohibitive for all but the simplest systems (this boundary is calculated in Chapter 2 for a very simple system). Second, even if the boundary could be determined, one must determine which portion of the boundary should be used when determining proximity of **p** to the boundary. Intuitively one might think that the boundary point closest in a Euclidean norm would be appropriate. However this point might correspond to an unreasonable **u**. For example u_i, corresponding to the MW output of a generator, is limited by the rating of that generator; it would be unreasonable to assume that this component of **u** could be an arbitrary value. With this context in mind, several of the techniques of determining proximity to voltage collapse are examined.

Probably the most common technique used by utilities today to maintain voltage security is the use of various operational guidelines and/or heuristic rules of thumb. These are based both upon studies performed days or months earlier using assumed system states and the individual operators "best judgement". An example operational guideline would be that utility A can only import X amount of power from utility B when A's load is Y, B's load is Z, and generator G_1 in utility C is out of service. While these guidelines have certainly proved useful in preventing some system problems, they have a number of fundamental

flaws. The main problem is that the guidelines are based on assumed conditions which never completely match the actual operating state. For example transmission lines or generators might be out of service, load distribution might not match what was anticipated, or neighboring utilities may be operating their systems in an unanticipated manner. Thus it is up to the system operator to determine how the limits in the guideline should be modified based upon actual conditions. Second, the guidelines do not provide any quantifiable indication of how close the system is to the voltage feasibility boundary. Thus the operator does not have a good idea of direction in which the state is moving, and how his actions are affecting the voltage security of the system. This information is particularly useful when unexpected operating states are encountered. Lastly, guidelines and rules of thumb can not be easily integrated into existing security enhancement software, which could then be used to restore the system to a secure operating point. Such software is normally based upon either a linear programming technique [5] or a Newton's method optimization [10]. Thus they are most easily adapted to use with easily differentiable voltage security measures.

A number of techniques have been developed which attempt to quantify how close the system is to the point of voltage collapse. These proximity indicators can be broken down into two groups: those that determine system voltage security by making assumptions about the future system trajectory from the present state, and those that use only information about the present state of the system.

The most straightforward of the former techniques is to simply make an assumption about how the system inputs will change with time and then solve the powerflow problem at a number of discrete timesteps until the simulated system loses its steady state solution (most techniques test for lack of solution by a Newton-Raphson iteration failing to converge). In essence a single point on the boundary is determined by making an estimate at the current time = t_0 of $\mathbf{u}(t)$ for $t > t_0$. The proximity to voltage collapse is then based upon the value of t when the critical point on the boundary is reached.

In normal circumstances utilities often have a fairly good idea of how some of the components of $\mathbf{u}(t)$, such as their own generation dispatch, their interchange with other companies and their customer load distribution, will vary over the next few hours. However there is often less certainty concerning the future variation of the generation, interchange, and load of their neighboring utilities (with whom they may have a competitive relationship). Additionally voltage collapse often occurs under abnormal circumstances

(such as under extremely high loads). In such situations the utility has little historical data upon which to base a prediction of future variations in **u**(t).

A problem with developing a proximity indicator based upon assumed future changes in **u** is that the indicator could be highly sensitive to the accuracy of this prediction of **u**. For example consider the case where the current operating point is close to the voltage stability boundary. If the assumed **u**(t) for $t > t_0$ moves the system state in a direction parallel to this boundary, the current operating point could be judged as quite secure. However, if the actual system moves in only a slightly different direction, the system could experience a voltage collapse. Additionally, since the calculation of this indicator requires a time simulation, it is not possible to calculate the effects of controller changes upon the proximity indicator without repeating the entire simulation from the new assumed operating point. This not only introduces additional inaccuracies due to again using an assumed **u**(t), but is computationally objectionable since each proposed controller change requires solving a series of powerflow solutions.

A number of improvements on this approach have appeared recently. In [11] the computational burden is reduced by recognizing that since the critical point of voltage collapse is characterized by singularity of the Jacobian, a critical point can be determined by solving the powerflow equations with the explicit requirement of singularity of the Jacobian matrix. This is accomplished by parameterizing **u** as a function of an arbitrary scalar t and then solving directly for the value of t which results in a singular Jacobian. The computational requirements of this method are quite modest (on the order of a single powerflow solution) and thus the method could be used on-line. In [12] the distance to voltage collapse is determined not by solving a series of powerflows, but rather through a series of linearized approximations. Thus this technique also results in reduced computational costs. Additionally, the results of various automatic control actions (such as transformer tap movement and generator reactive saturation) which would occur along the simulated trajectory can be included. However as with the earlier method, the resultant accuracy of both these techniques depends upon the appropriateness of the calculated boundary point. Also, neither of these proximity measures is determined with an easily differentiable function, and thus it could be difficult to calculate sensitivities of the proximity measure to the actions of the various controllers.

In [13] an approach is presented which attempts to determine the closest point on the feasibility boundary. This point is determined through an iterative process where each

successive value of $\mathbf{u}(t)$ is determined by moving in the direction of the gradient of the determinant of the powerflow Jacobian. The boundary is assumed to be reached when the value of the determinant is sufficiently small. By providing a result based upon the distance to the closest boundary point, the technique is not dependent upon an assumed $\mathbf{u}(t)$. However, the authors state that the calculation of $\nabla|\mathbf{J}|$ is very time consuming, with the computational cost greater than $O(n^3)$ (where n is the number of buses in the power system model).

The other major grouping of methods of assessing proximity to voltage instability are those techniques which only use information about the present state of the electrical system. In contrast to the previously discussed methods, they make no assumptions about future system trajectories.

Many authors have proposed singularity of the Jacobian of the powerflow equations as a test for the onset of voltage collapse. In particular, [14] recommends the use of the smallest singular value of the Jacobian of the powerflow equations, denoted by σ_{min}, as a proximity indicator. The singular value of the Jacobian matrix $\mathbf{J}$ is defined as the square root of the smallest eigenvalue of $(\mathbf{J}^T\mathbf{J})$. As the system moves towards the point of voltage collapse, σ_{min} decreases, eventually reaching zero when $\mathbf{J}$ becomes singular. The proposed method of enhancing system security is to move controllers so that σ_{min} is maximized while maintaining feasibility. In order to perform this optimization, it is necessary to calculate the sensitivity of σ_{min} to each of the system controllers. This is done using a singular value decomposition of the Jacobian matrix.

The advantage of this approach is that it is not necessary to make predictions about future changes in the system trajectory. The proximity indicator is solely based upon the current operating point. Additionally, the calculation of σ_{min} is not extremely computationally expensive. This is because for a large system it is possible to take advantage of the sparsity of $(\mathbf{J}^T\mathbf{J})$ when calculating σ_{min}. However the method does have a number of disadvantages. First, the sensitivity of σ_{min} to changes in the system state can be high near the point of voltage collapse, yet relatively low else where. This could cause problems as a system gradually approaches the point of voltage collapse, since σ_{min} might vary slowly initially, giving the operator a false sense of security. The value may only begin to rapidly decrease when voltage collapse is imminent and it is too late for preventative controller actions. An example of such a scenario is shown in [34]. Second, since σ_{min} is only based upon the current operating point, important power system nonlinearities such as

generator saturation and transformer tap limits are not considered. These effects can often be crucial in determining the ultimate point of voltage collapse. Last, the computational cost of computing the singular value decomposition of the Jacobian matrix is $O(n^3)$ Therefore it is computationally prohibitive for a large system, at least on a serial machine. In [15] a singular value decomposition algorithm is presented using large arrays of parallel processors. Whether such an approach is workable in a utility control center has yet to be determined.

A different type of indicator, which is also only based upon the current operating state, is presented in [16]. The proposed qualitative measure varies from 0 (for a system with no load) to 1 for a system experiencing voltage collapse. The measure is calculated by partitioning the bus admittance matrix based upon load and generator buses. Then a partial inversion of the matrix is performed in order to calculate the load bus voltages as a linear function of their currents and the generator bus voltages. A security measure L_j is then calculated for each bus based upon these linearizations. The system security indicator is the maximum of the L_j's.

This indicator has the advantage that it can be obtained with reasonable computational effort and can be extended to large systems. One of the difficulties with the approach is that since only current operating point information is used, the nonlinear effects of generators and transformers can not be included unless the devices have already hit their limits at the current operating point. Also it appears that it would be difficult to derive the effects of controller actions on the measure in order to improve system voltage security.

A variation of the use of Jacobian singularity to determine proximity to voltage collapse is presented in [17] and [33]. Rather than using the least singular value of the Jacobian, three security measures are calculated. First, an estimate of the eigenvalue of the portion of the Jacobian matrix associated with the reactive power equations at the load buses is calculated. This eigenvalue estimate is based upon the flows in the system, and measures the reactive power surplus or deficit of the transmission system. For a secure system the eigenvalue is very large, becoming smaller as the system load is increased. Second, the ability of the voltage control devices in a portion of the system to maintain voltage controllability is determined. A system has voltage controllability if it is possible to both raise the voltage at the load buses by increasing the generator voltage set points, and if decreasing the reactive load causes an increase in the bus voltages. These sensitivity values are based upon selective values of the inverse of the Jacobian matrix. Once all the voltage control devices

within an area have reached their limits, the area no longer has voltage controllability. The third security criteria is based upon the amount of reactive power which can be imported into an area with a reactive deficiency. This value is a measure of the reactive transmission reserve on the boundary of the voltage vulnerable area.

A third major grouping of voltage collapse proximity indicators are the methods based upon multiple solutions of the system equations. As will be shown in later sections, these methods can be thought of as a hybrid between the methods which dependent explicitly upon an assumed future system trajectory, and those that use only current system state information. Techniques utilizing multiple solutions include the energy based approach, which is the subject of this thesis proposal, and the methods presented in [30] and [18]. The latter methods are based upon calculating a scalar index which can be interpreted as the "angle" between two of the vector solutions of (1-2). These indices will be discussed in greater detail in later sections. The former technique will, of course, be covered in great detail in this proposal.

As has been shown, a number of different approaches have been put forth to determine the voltage vulnerability of power systems. While many of these approaches have provided insight into the voltage instability problem, no technique to date has provided the electric utilities with an easily computable, accurate measure which can be used both to determine how close a system is to voltage instability, and how to best increase the system voltage security. In this thesis proposal a method based upon energy function techniques is proposed to solve these two problems.

Chapter 2 - Application of Energy Function Methods to Voltage Collapse

2.1 Energy Function Methods Introduced

The problem of voltage instability is closely related to the study of the region of attraction of an autonomous nonlinear system with an asymptotically stable equilibrium. One tool which has proved useful in analyzing the region of attraction of such systems is Lyapunov's direct method. Consider a set of differential equations of the form

$$\dot{\mathbf{x}} = \mathbf{f}(\mathbf{x}) \tag{2-1}$$

Comparing this equation with (1-1) we note that $\mathbf{u}(\bullet)$ is no longer explicitly identified and the algebraic variables have been eliminated. This is not to say that $\mathbf{u}(\bullet)$ is longer present, but rather that it is modeled as a fixed known input. The idea behind Lyapunov's direct method is that for a time invariant system of the form of (2-1), with an equilibrium point $\mathbf{x}^s$, it is possible to develop sufficient conditions for the stability of $\mathbf{x}^s$, if one can define a function ϑ which is in some sense analogous to "energy" of the system. Typical requirements on such a function are that $\vartheta(\mathbf{x}^s) = 0$ and ϑ is a locally positive definite function (l.p.d.f.) about the stable equilibrium over some region (Ω). The energy derivative along trajectories of the system is defined as

$$\dot{\vartheta}(\mathbf{x}) = \nabla\vartheta(\mathbf{x})\, \mathbf{f}(\mathbf{x}(t)). \tag{2-2}$$

Then if the system dynamics are such that $\dot{\vartheta}(\mathbf{x})$ is always less than or equal to zero for all ($\mathbf{x} \in \Omega$) (so that the energy is non-increasing with time) and eventually reaches zero, then we expect that $\mathbf{x}^s$ is asymptotically stable. Additionally, ($\forall \mathbf{x} \in \Omega$) are contained within the region of attraction of $\mathbf{x}^s$. These results can be stated formally as LaSalle's theorem [19]:

LaSalle's Theorem Suppose the system in (2-1) is autonomous. Let $\vartheta: R^n \rightarrow R$ be a continuously differentiable l.p.d.f., and suppose that for some $\vartheta^{cr} > 0$, the set

$$\Omega_c = \text{component of } \{\mathbf{x} \in R^n : \vartheta(\mathbf{x}) \leq \vartheta^{cr}\} \text{ containing } \mathbf{x}^s$$

connected region *

is bounded. Suppose ϑ is bounded below on Ω_c, that $\dot{\vartheta}(\mathbf{x}) \leq 0 \; \forall \mathbf{x} \in \Omega$, and that the set

$$S = \{\mathbf{x} \in \Omega_c : \dot{\vartheta}(\mathbf{x}) = 0\}$$

contains no trajectories of (2-1) other than the trivial trajectory $\mathbf{x}(t) \equiv \mathbf{x}^s$. Then the equilibrium point $\mathbf{x}^s$ of (2-1) is asymptotically stable.

Thus Ω can be thought of as defining an energy "well". Unless the system receives a disturbance that pushes the state to a point with energy greater than ϑ^{cr}, the state can not escape the well and will eventually return asymptotically to $\mathbf{x}^s$. LaSalle's theorem can be applied to power systems by first assuming that the system is time invariant. This corresponds to freezing $\mathbf{u}^{slow}(t) = \hat{\mathbf{u}}$ (constant) and setting $\mathbf{u}^{small} \equiv \mathbf{0}$. Then, assuming that a suitable ϑ function can be defined, we can think of the stable operating point of the system as being close to the bottom of a time invariant energy well with the "depth" of the well determined by both $\hat{\mathbf{u}}$ and the system equations. The depth of the well gives us some indication of the security of the current operating point since the greater the depth, the larger the "kick" needed to escape the well. This depth can be measured by calculating the energy associated with the lowest point(s) on the boundary of the well. A necessary condition for such a saddle point is that $\nabla\vartheta(\mathbf{x}) = 0$; it will be shown later that for the energy function used here that these saddle points correspond to the unstable equilibrium points (UEPs) of (2-1).

The use of energy functions has recently proved quite useful in determination of system transient stability [20]. In that context, a large disturbance is first applied to the system, which, in essence, gives the system some initial "energy". Following the disturbance, a time invariant system model is assumed, so the existence of a time invariant energy well follows. Using the simplest Lyapunov based criterion, if the initial energy following the disturbance is less than that of the UEP of the post-fault system with the lowest energy, the system will asymptotically return to its post-fault equilibrium point. Other more sophisticated criterion make use of such concepts as the "controlling UEP" or "potential energy boundary surface." These approaches recognize that a fault which yields a system trajectory passing exactly through the lowest saddle point is a rare, worst case scenario.

In the voltage security problem, as noted earlier, the system has either not been subject to a large disturbance, or has seemingly "settled down" following the disturbance. However

the system is subject to a time varying input $\mathbf{u}(\bullet)$ with a time scale of minutes to hours, which is not known precisely beforehand. Therefore the operating point of the system is moving in a "quasi-static" manner. The "frozen" equilibrium point only approximates the true state of the system. At any fixed time $\hat{t}$ the shape of the energy well about the frozen equilibrium point could be determined. However the key point is that this energy well is also a function of time, since its boundaries are at least partially a function of the operating point. As the system moves closer to the point of voltage collapse one would expect the height of the energy well to decrease. This will be shown to be the case in later sections. Eventually at the point of voltage collapse, where a stable solution no longer exists, the height of the well would be zero. Thus while the system has always remained close to the bottom of the well (close to its frozen equilibrium point), the shape of the well has changed with time so that at voltage collapse the energy function about this point is no longer locally positive definite. In actuality, however, shortly before this point the random load variations, which have little effect on a normal, robust operating point, will dominate and cause the state to escape from the now shallow well. Once the state leaves the potential well about the operating point, the deterministic dynamics drive a very rapid decline in voltage magnitudes until either the problematic portion of the system is isolated by protective relaying actions, or the entire system collapses.

2.2 Derivation of Energy Function for Voltage Stability Assessment

The energy function method will first be developed by examining the static powerflow in a single line example. Consider the system shown in Figure 2-1. For simplicity the transmission line will be assumed to be lossless so that the real power injection at bus 1 must equal the real load at bus 2. Furthermore assume that the load attached to bus 2 is represented by a constant P-Q demand. The resulting power balance equations at bus 2 are:

$$P_L + B_{12}V\sin(\alpha) = 0 \tag{2-3}$$

$$Q_L - B_{22}V^2 - B_{12}V\cos(\alpha) = 0 \tag{2-4}$$

where

V := bus voltage magnitude at bus 2

$\alpha := \delta_2 - \delta_1$ phase angle difference between bus 2 and bus 1

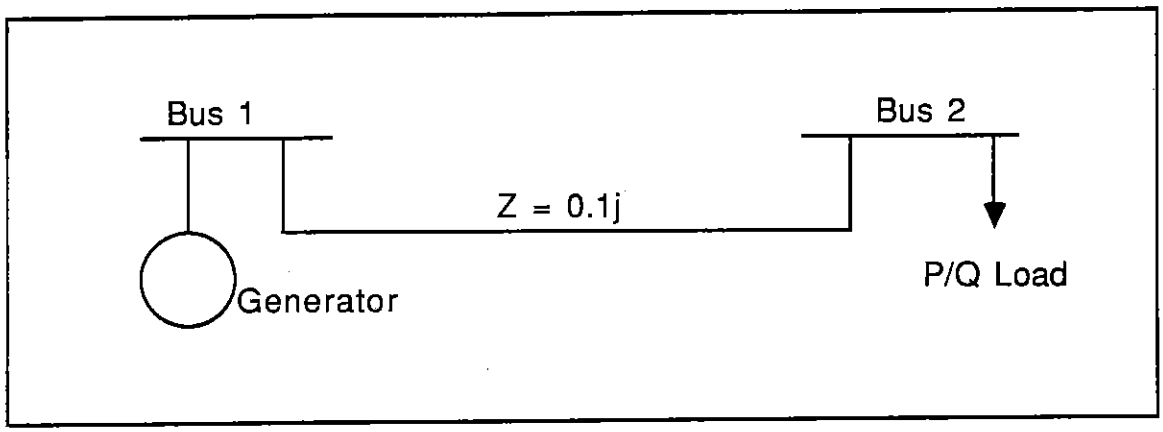

Figure 2-1 : One-line Diagram of Two Bus System

For $B_{12} = -B_{22} = 10.0$, the locus of points in the α-V space satisfying these constraints for a range of P and Q values are shown in Figure 2-2. A radial line with a fixed sending voltage typically has two solutions for receiving end voltage. This is reflected in Figure 2-2 by the fact that the P and Q constraints typically have two intersections, each corresponding to a powerflow solution. However, as shown in Figure 2-2, for certain critical values of P and Q, the two constraint curves become tangent, with only one resultant solution. If either P or Q is increased further, the powerflow equations no longer have a solution. At this point the Jacobian of the two power balance equations must be singular.

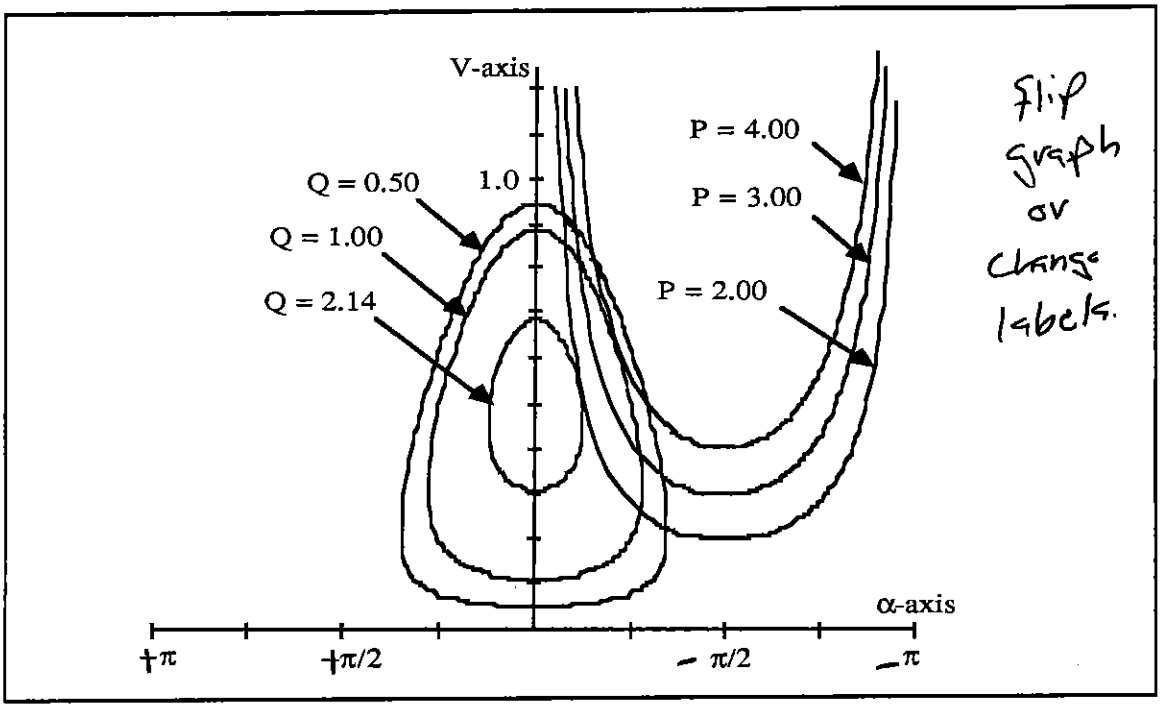

Figure 2-2 : Power Balance Constraints in α-V Plane

In order to develop the energy function approach, it is necessary to also introduce dynamics to augment the algebraic powerflow equations. Note that the dynamics in this example do not represent the most general models that can be accommodated by the method. The goal here is to illustrate the basic methodology; the range of allowable models will be discussed later. First assume that the real power demand at bus 2 is a constant plus a linear term dependent on bus frequency. This follows the structural preserving model introduced for transient stability analysis in [21]. Using the classical model for the generator, the system equations are then given by:

$$M_g\dot{\omega} + D_g\omega - B_{12}V\sin(\delta_1-\delta_2) - P_M = 0$$

$$-(P_L + D_l\dot{\delta}_2) = B_{12}V\sin(\delta_2-\delta_1)$$

$$-Q_L = -B_{22}V^2 - B_{21}V\cos(\delta_2-\delta_1)$$

Under the assumptions that $|P_M| = |P_L|$ (generator mechanical power matches active load demand) and $B_{12} = B_{21}$, and recalling the definition of α, these may be rewritten as:

$$\dot{\omega} = -M_g^{-1}D_g\omega - M_g^{-1}f(\alpha,V) \tag{2-5a}$$

$$\dot{\alpha} = -D_l^{-1}f(\alpha,V) + \omega \tag{2-5b}$$

$$0 = V^{-1}g(\alpha,V) \tag{2-5c}$$

where

M_g = Inertia constant of the generator

D_l, D_g = Damping of load and generator

$f(\alpha,V) := P_L + B_{12}V\sin(\alpha)$

$g(\alpha,V) := Q_L - B_{12}V\cos(\alpha) - B_{22}V^2$

Note that multiplication by V^{-1} in (2-5c) does not affect the desired solutions because voltage magnitudes are always restricted to be strictly positive. The equilibrium of (2-5) are the (α,V) intersection points pictured in Figure 2-2, in the ω=0 plane.

The mixed system of differential and algebraic constraints in (2-5) is not guaranteed to define a globally well posed dynamical system. That is to say that for some feasible initial conditions trajectories cannot be continued for all time, particularly when the voltage magnitudes are very low [22]. However, using the technique from [22] the algebraic equation is singularly perturbed to form a differential equation whose equilibrium is the solution of the original equation. For (2-5c), this becomes

$$\varepsilon\dot{V} = -V^{-1}g(\alpha,V) \tag{2-5d}$$

where ε is a small positive parameter that controls the speed with which trajectories of voltage magnitude move towards values satisfying the reactive power balance. We will show later that the model's ability to predict voltage collapse is independent of the choice of this parameter. From an engineering standpoint, 2-5d may be interpreted as follows. The reactive load demand is taken as an "independent input", and the voltage magnitude

responds to this input to maintain reactive power balance. The right-hand side of 2-5d is the difference between the reactive power absorbed by the load and the reactive power delivered to the load. When the load instantaneously demands more reactive power than the system is supplying, (2-5d) predicts that the bus voltage drops until power balance is re-established. The rate of this change is dependent upon ε; for ε sufficiently small it is essentially instantaneous and the behavior is nearly identical to the original algebraic equation. Note that the use of ε is not advocated for simulating system trajectories since this would create an unnecessarily stiff set of differential equations to be solved. The point of introducing (2-5d) is to obtain a single model that is physically reasonable over a wide operating range of voltage, thereby facilitating the energy function analysis.

In order to develop the energy function for the system of equations given by (2-5a), (2-5b) and (2-5d), we first write them in matrix form as

$$\begin{bmatrix} \dot{\omega} \\ \dot{\alpha} \\ \dot{V} \end{bmatrix} = \begin{bmatrix} -M_g^{-1}D_gM_g^{-1} & -M_g^{-1} & 0 \\ M_g^{-1} & -D_l^{-1} & 0 \\ 0 & 0 & -\frac{1}{\varepsilon} \end{bmatrix} \begin{bmatrix} M_g\omega \\ f(\alpha,V) \\ V^{-1}g(\alpha,V) \end{bmatrix} \qquad (2\text{-}6)$$

with M_g,D_l,D_g and ε assumed to be strictly positive.

Defining $\mathbf{A}$ as the 3 by 3 matrix from the right hand side of (2-6), $\mathbf{x} = [\omega\ \alpha\ V]^T$, and letting $\theta(\mathbf{x})$ be defined as the vector function of the right-hand sides of equations (2-5a), (2-5b) and (2-5d), we can derive a Lyapunov function for this system using the following theorem:

Theorem 2.1 [23]

Suppose the system of the form $\dot{\mathbf{x}} = \theta(\mathbf{x})$ has a strictly stable linearization at the equilibrium point $\mathbf{x}^s$. Further if there exists a constant matrix $\mathbf{A} \in R^{nxn}$, such that

a) $\det(\mathbf{A}) \neq 0$;

b) $(\mathbf{A}+\mathbf{A}^T) \leq 0$, i.e., $(\mathbf{A}+\mathbf{A}^T)$ is negative semi-definite;

c) $\mathbf{A}^{-1}\theta(\mathbf{x}) = \nabla\vartheta(\mathbf{x})$ is a gradient function, or equivalently,

$$\nabla^2\vartheta(\mathbf{x}) = \frac{\partial^2\vartheta(\mathbf{x})}{\partial\mathbf{x}^2} = \mathbf{A}^{-1}\frac{\partial\theta(\mathbf{x})}{\partial\mathbf{x}} \text{ is symmetric}$$

Under these conditions the integral

$$\vartheta(\mathbf{x}) = \int_{\mathbf{x}^s}^{\mathbf{x}} [\mathbf{A}^{-1}\theta(\mathbf{x})]^T d\mathbf{x} \tag{2-7}$$

defines a Lyapunov function for the system of (2-1), i.e., $\vartheta(\mathbf{x})$ is locally positive definite about $\mathbf{x}^s$, and

$$\dot{\vartheta}(\mathbf{x}) = [\nabla\vartheta(\mathbf{x})]^T\theta(\mathbf{x}) = \frac{1}{2}[\nabla\vartheta(\mathbf{x})]^T(\mathbf{A}+\mathbf{A}^T)\nabla\vartheta(\mathbf{x}) \le 0.$$

For the power system under consideration, the initial stipulation that (2-6) have a strictly stable linearization at the equilibrium point $\mathbf{x}^s$ is met by definition because only systems which have steady state stability are studied. The first requirement that $\det(\mathbf{A}) \neq 0$ can be shown to be true by straightforward calculation. Second, $(\mathbf{A}+\mathbf{A}^T)$ can be shown to be negative semi-definite by noting that it is a diagonal matrix whose diagonals are all < 0. Lastly,

$$\mathbf{A}^{-1}\frac{\partial\theta(\mathbf{x})}{\partial\mathbf{x}} = \begin{bmatrix} M_g & 0 & 0 \\ 0 & B_{12}V\cos(\alpha) & \sin(\alpha) \\ 0 & \sin(\alpha) & -\frac{Q_L}{V^2} - B_{22} \end{bmatrix}$$

is a symmetric matrix, implying that $\mathbf{A}^{-1}\theta(\mathbf{x})$ is a gradient function. Therefore it is possible to define $\vartheta(\mathbf{x})$ by (2-7). By definition $\vartheta(\mathbf{x})$ is dependent not only upon $\mathbf{x}$ but also upon $\mathbf{x}^s$ and can be characterized as an "energy difference" between the two states. However since the power systems under consideration here are assumed to have only a single stable equilibrium point of interest (the normal operating state of the system), for notational simplicity this dependence on $\mathbf{x}^s$ will be made to be implicit. Note also that since $\mathbf{A}$ is nonsingular, equilibrium of (2-6) only occur at those points where

$$\nabla\vartheta(\mathbf{x}) = \mathbf{A}^{-1}\theta(\mathbf{x}) = 0.$$

Formally, the previous definition of the Lyapunov function $\vartheta(\mathbf{x})$ is sufficient to show stability of $\mathbf{x}^s$ in the sense of Lyapunov, but not asymptotic stability. This is because we have not precluded the set

$$\Omega_c = \text{component of } \{x \in R^n : \vartheta(\mathbf{x}) \le \vartheta^{cr}\} \text{ containing } \mathbf{x}^s$$

from containing trajectories of (2-1) where $\dot{\vartheta}(\mathbf{x}) \equiv 0$. If such a trajectory were to exist, the value of $\vartheta(\mathbf{x})$ would never decay to zero, indicating that $\mathbf{x}$ is not converging to $\mathbf{x}^s$. However if $(\mathbf{A}+\mathbf{A}^T)$ is negative definite, then Ω_c does not contain any trajectories where $\dot{\vartheta}(\mathbf{x}) \equiv 0$ (other than the trivial trajectory $\mathbf{x}(t) \equiv \mathbf{x}^s$), and asymptotic stability can be shown by LaSalle's theorem. This will be the case if all the diagonal elements of $\mathbf{A}$ are strictly less than zero.

For the two bus system under consideration here, with an equilibrium point $(0,\alpha^s,V^s)$, the Lyapunov function $\vartheta(\omega,\alpha,V)$ is given in closed form by:

$$\vartheta(\omega,\alpha,V) := \frac{1}{2}M_g\omega^2 - B_{12}V\cos(\alpha) + B_{12}V^s\cos(\alpha^s)$$

$$-\frac{1}{2}B_{22}V^2 + \frac{1}{2}B_{22}(V^s)^2 + P_L(\alpha-\alpha^s) + Q_L \ln\left(\frac{V}{V^s}\right) \qquad (2\text{-}8)$$

Using (2-8) it is possible to calculate the energy difference between any point in the (ω,α,V) space and the stable equilibrium point $\mathbf{x}^s$. For example, if we let P = 200MW and Q = 100MVAR, the per unit stable equilibrium point (i.e. the standard powerflow solution) is (0,-13.52°,0.855). This solution can be verified by straightforward substitution into (2-6); note that the equilibrium point is independent of the values of the elements of $\mathbf{A}$. Figure 2-3 plots the contours of this energy difference in the $\omega = 0$ plane. Similar plots could, of course, be produced for $\omega \neq 0$.

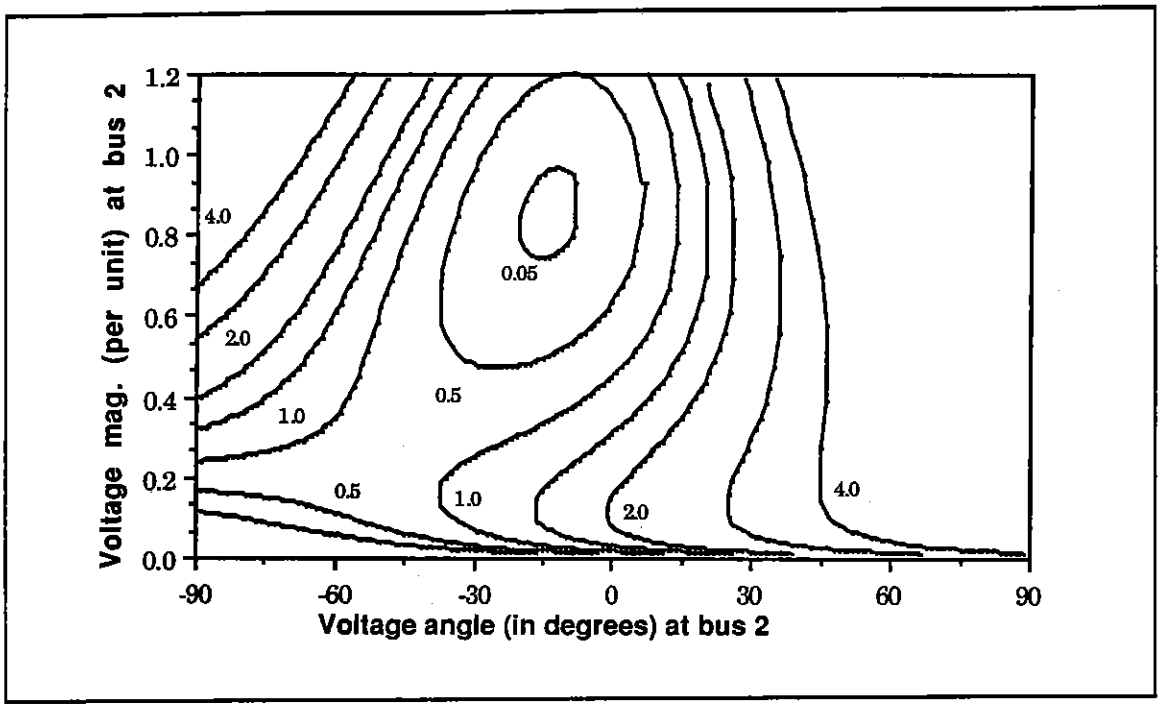

Figure 2-3 : Contours of Energy Function ϑ in α-V Space

To determine the depth of the energy well, it is necessary to calculate the value of the "nearest" saddle point, where $\nabla\vartheta(\mathbf{x}) = 0$. Geometrically, this is the first point $\mathbf{x}$, satisfying $\nabla\vartheta(\mathbf{x}) = 0$, encountered by expanding constant contours of ϑ from $\mathbf{x}^s$. As noted earlier, this can only occur at equilibrium points of (2-6). For the simple two bus system under consideration here, it is shown in [24] that such a system only has at most two equilibrium points and therefore at most one saddlepoint. The equilibrium points correspond to the intersection of the two constraints shown in Figure 2-2. For the example loads of the previous paragraph, this second equilibrium is at (0, -49.91°, 0.261). The energy difference for this system this then found using (2-8) to be 0.8608.

The steady-state stability of each of these equilibrium points can be calculated by linearizing the system about each point and then determining the eigenvalues. The linearized equations are given by

$$\begin{bmatrix} \dot{\omega} \\ \dot{\alpha} \\ \dot{V} \end{bmatrix} = \begin{bmatrix} -M_g^{-1}D_g & -M_g^{-1}\frac{\partial f(\alpha,V)}{\partial \alpha} & -M_g^{-1}\frac{\partial f(\alpha,V)}{\partial V} \\ 1 & -D_l^{-1}\frac{\partial f(\alpha,V)}{\partial \alpha} & -D_l^{-1}\frac{\partial f(\alpha,V)}{\partial V} \\ 0 & \frac{1}{\varepsilon}\frac{\partial [V^{-1}g(\alpha,V)]}{\partial \alpha} & \frac{1}{\varepsilon}\frac{\partial [V^{-1}g(\alpha,V)]}{\partial V} \end{bmatrix} \begin{bmatrix} \Delta\omega \\ \Delta\alpha \\ \Delta V \end{bmatrix} \quad (2\text{-}9)$$

Define the above matrix as **A**. An analytic calculation of the individual eigenvalues of the above system would be quite difficult. Nevertheless, a number of properties concerning the stability of the above system can be determined analytically. Throughout the following analysis it will be assumed that M_g, D_g, D_l and ε are all strictly positive. The requirement that the generator inertia and damping constants, M_g and D_g, are strictly positive is satisfied for realistic generator models. The requirement that the load parameters, D_l and ε, are also strictly positive is based upon realistic load models and is normally satisfied in practice.

Note that at an equilibrium point [where $g(\alpha,V) = 0$ by definition],

$$\frac{\partial [V^{-1}g(\alpha,V)]}{\partial V} = V^{-1}\frac{\partial g(\alpha,V)}{\partial V})$$

Define

$$J_1 = \frac{\partial f(\alpha,V)}{\partial \alpha}$$

$$J_2 = \frac{\partial f(\alpha,V)}{\partial V}$$

$$J_3 = \frac{\partial g(\alpha,V)}{\partial \alpha}$$

$$J_4 = \frac{\partial g(\alpha,V)}{\partial V}$$

$J_{pf} = J_1J_4 - J_2J_3 =$ Determinant of Jacobian of (2-3) and (2-4) = Powerflow Jacobian

$$c_1 = D_1^{-1}J_1 + (V\varepsilon)^{-1}J_4$$

$$c_2 = (M_g^{-1}D_g(D_1V\varepsilon)^{-1} + M_g^{-1}(V\varepsilon)^{-1})$$

The characteristic equation of **A** is then given by

$$\lambda^3 + (c_1+M_g^{-1}D_g)\,\lambda^2 + (M_g^{-1}D_gc_1 + (D_1V\varepsilon)^{-1}J_{pf}+M_g^{-1}J_1)\,\lambda + c_2\,J_{pf} \qquad (2\text{-}9a)$$

The roots of the characteristic equation (2-9a) then determine the matrix's eigenvalues. The Routh-Hurwitz stability criterion can be used to determine the stability of the system [39]. Define the Routh array for (2-9) as

Column 1	Column 2
1	$(M_g^{-1}D_gc_1+M_g^{-1}J_1+(D_1V\varepsilon)^{-1}J_{pf})$
$(c_1+M_g^{-1}D_g)$	$c_2\,J_{pf}$
$\dfrac{(M_g^{-1}D_gc_1+M_g^{-1}J_1)\,(c_1+M_g^{-1}D_g) + (c_1D_1^{-1} - M_g^{-1})(V\varepsilon)^{-1}J_{pf}}{c_1+M_g^{-1}D_g}$	0
c_2J_{pf}	0

Proposition (sufficient conditions for system stability)

A necessary and sufficient condition for stability is that there are no changes of sign in the elements in the first column of the Routh Array. Since the element in the first row is 1, all the elements in this column must be positive. The following are sufficient conditions for the stability of system (2-9):

1. M_g, D_g, D_l , V and ε are all strictly positive.
2. J_1 and J_4 positive
3. $J_2 * J_3$ be non-negative
4. $J_{pf} > 0$

Proof

The first element in row 2 is positive by assumptions 1 and 2. This is because J_1, J_4 ,D_l , V and ε positive implies $c_1 > 0$. A sufficient condition for the first element in row 3 to be positive is that $J_2 * J_3$ be non-negative. The denominator is positive by the previous argument. The numerator can be rewritten as

$$(M_g^{-1}D_g c_1 + M_g^{-1}J_1)\, M_g^{-1}D_g + M_g^{-1}D_g c_1^2 + M_g^{-1}J_1\ D_l^{-1}J_1 + c_1 D_l^{-1}(V\varepsilon)^{-1}J_{pf} +$$
$$M_g^{-1}(V\varepsilon)^{-1}J_1J_4 - M_g^{-1}(V\varepsilon)^{-1}J_1J_4 + M_g^{-1}(V\varepsilon)^{-1}J_2J_3$$

Canceling the second and third to last terms results in an expression with all terms strictly positive except for the last term, which is non-negative by assumption 3. The first element in row 4 is positive by assumptions 1 and 4. ♦

From (2-3) and (2-4) it can be seen that assumption 2 is satisfied if the angle across the transmission line is less than 90 degrees with B_{12} positive and B_{22} negative. These assumptions are almost always satisfied in practice. Assumption 3 is always satisfied for the lossless case under consideration here because

$$\frac{\partial f(\alpha,V)}{\partial V} = V^{-1}\frac{\partial g(\alpha,V)}{\partial \alpha}$$

Therefore we can conclude that for a "normal" (defined as when assumptions 1 through 3 hold) lossless two bus system, a sufficient condition for stability is that the determinant of the powerflow Jacobian is positive.

Proposition (sufficient conditions for system instability)

The following are sufficient conditions for instability of system (2-9):

1. M_g, D_g, D_l , V and ε are all strictly positive.
2. $J_{pf} < 0$

Proof

By the Routh-Hurwitz stability criterion, the number of sign changes in elements of the first column of the Routh array determines the number of eigenvalues with strictly positive real parts. Since the first element in the first row is positive ("1"), we only need show that at least one element in the first column is negative. Since $J_{pf} < 0$ by assumption 2 and $c_2 > 0$ by assumption 1, the first element in the last row is negative. ♦

Proposition (system [2-9] can only lose stability by eigenvalues passing through origin)

Provided M_g, D_g, D_l , V and ε are all strictly positive, the system from (2-9) can not have purely imaginary eigenvalues (other than the trivial case of eigenvalues at the origin) when there are no other eigenvalues in the right half plane. Equivalently, the only way the system can lose stability is for an eigenvalue to pass from the left half plane through the origin into the right half plane.

Proof

Assume the opposite, that the system loses stability by a pair of complex conjugate eigenvalues moving into the right half plane, not passing through the origin. At the point where they cross the imaginary axis, $|\mathbf{A}| \neq 0$ since $|\mathbf{A}|$ is equal to the product of the matrix's eigenvalues and we have assumed that the system does not have a zero eigenvalue. However a necessary and sufficient condition for $|\mathbf{A}| \neq 0$ is that $J_{pf} \neq 0$ since

$$|\mathbf{A}| = -J_{pf}\left(M_g^{-1}D_g(D_1V\varepsilon)^{-1} + M_g^{-1}(V\varepsilon)^{-1}\right)$$

However if $J_{pf} > 0$ all the eigenvalues have negative real parts, contradicting the original assumption that a pair of complex conjugate eigenvalues are on the imaginary axis. Conversely if $J_{pf} < 0$ the system is unstable, contradicting the assumption that a stable system is losing stability. Thus we've established a contradiction since we originally assumed that $J_{pf} \neq 0$. ♦

Therefore for the two bus lossless system the stability of the equilibrium point can be determined by the sign of the determinant of the powerflow Jacobian. For the second equilibrium point (0, -49.91°, 0.261) from above, the determinant of the Jacobian is -17.3, so the equilibrium point is unstable. This unstable equilibrium point (UEP) will be referred to as the low voltage solution. Since from (2-2) $\dot{\vartheta}(\mathbf{x}) = 0$ at an equilibrium point, the value of the energy difference at this UEP, $\vartheta(0, -49.91°, 0.261)$, can be used to measure the depth of the energy well.

The ability of the energy difference to predict vulnerability of a system to voltage collapse for the two bus system will be examined next. The question to be answered is for a given P/Q load value, how much more load can be added before voltage collapse occurs. As was mentioned earlier, the system will loss steady state stability when the Jacobian of the two power balance equations is singular. Geometrically, this singular solution occurs when the active and reactive power constraint curves are tangent to one another. If either P or Q is increased further, the curves no longer intersect, and the powerflow has no solution.

For the 2 bus system it is possible to derive the algebraic expression describing the locus of points in the (P,Q) space where the Jacobian is singular. First observe that the Jacobian for the system is

$$\mathbf{J} = \begin{bmatrix} B_{12}V\cos(\alpha) & B_{12}V\sin(\alpha) \\ B_{12}V\sin(\alpha) & -2B_{22}V - B_{12}V\cos(\alpha) \end{bmatrix}$$

Points of singularity are identified by setting the determinant to zero, yielding the constraint

$$\det(\mathbf{J}) = V\,(-2B_{12}B_{22}V\cos(\alpha) - (B_{12})^2) = 0$$

Ignoring the case of V = 0, the determinant is zero for all (α,V) pairs satisfying

$$V\cos(\alpha) = \frac{-B_{12}}{2B_{22}}$$

Since each point in the (α,V) space maps to only one point in the (P,Q) space, the locus of points which satisfy the above equation can be plotted in the (P,Q) space. These points are shown in Figure 2-4. Note that the boundary between the feasible and infeasible regions is only a function of the system parameters B_{12} and B_{22}. Since the boundary is defined as the set of loads whose constraint curves are tangent, each point on the boundary has only a single powerflow solution. Hence the energy difference associated with these points is identically zero since the upper and lower limits of the integral in (2-7) are equal. For each point contained within the feasible region, an energy difference can be calculated by first determining both the normal operating point solution and the low voltage solution, and then calculating the energy difference using (2-7). The contours of these energy differences are shown in Figure 2-5. Since those points in the infeasible region do not contain a stable equilibrium point, there is no corresponding energy well, and thus the energy difference is not defined.

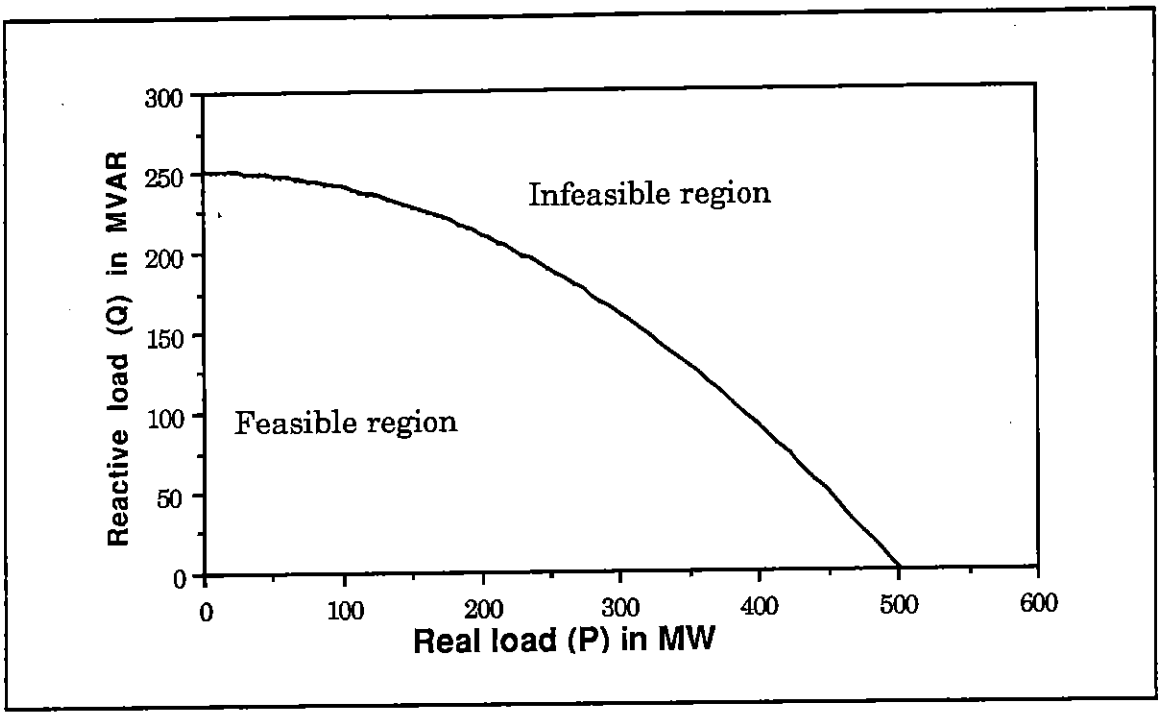

Figure 2-4 : Locus of Points where Powerflow Jacobian is Singular

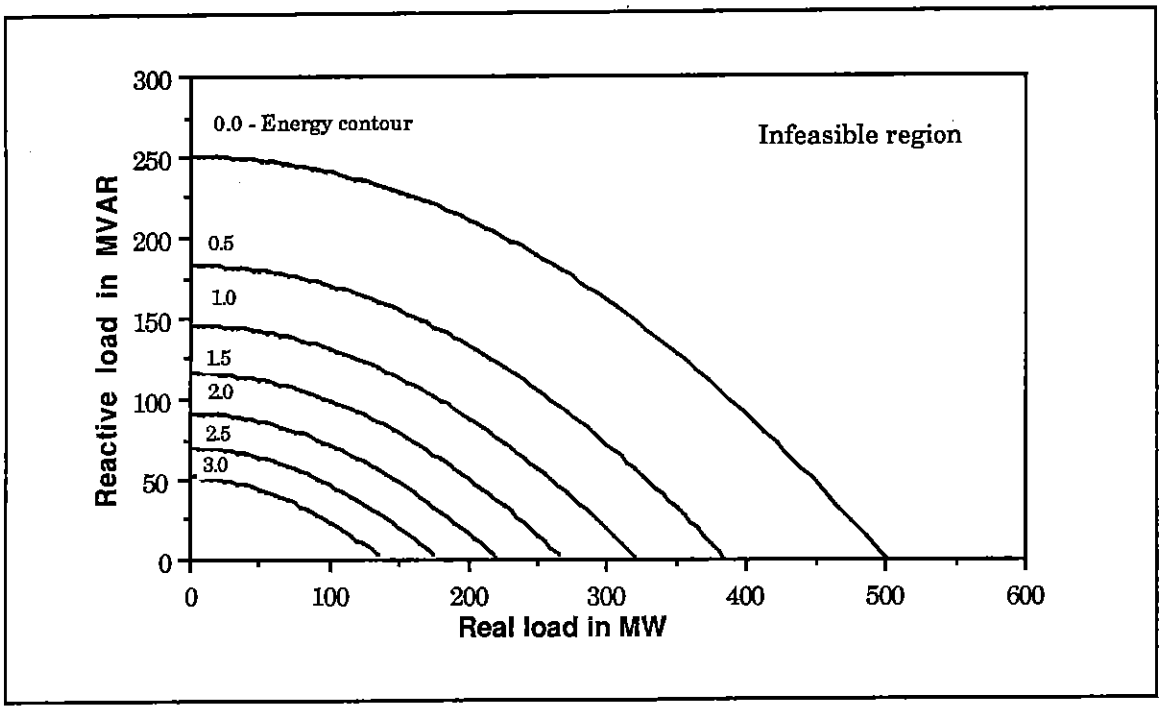

Figure 2-5 : Contours of Energy Function ϑ in P-Q Space

Interestingly, the energy contours in Figure 2-5 are both parallel to the feasible region boundary and fairly evenly spaced. Recognizing this, various frozen equilibrium points (operating states) could be ranked, according to their proximity to the feasible region boundary, by their corresponding energy difference. The usefulness of this method's ability to rank operating points is illustrated in the following example. Consider a fairly typical scenario where P(t) and Q(t) are slowly varying functions of time which are not known a priori. Also assume that the operating point is sampled at a rate so that relatively small variations in P and Q occur between sample periods. At each sample period we'd like to calculate a proximity index which tells us how close the system is to voltage collapse so that corrective action can be taken if needed.

For such an approach to provide useful results, a number of criteria are needed of the proximity index. First, we need to know beforehand what value of the index corresponds to voltage collapse. Therefore a simplistic approach of watching the voltage magnitude at the load bus would not work since we have no idea beforehand of the voltage magnitude at which voltage collapse will occur. The energy method provides this functionality since voltage collapse occurs by definition when the energy difference is zero. Second, in order for the proximity index to adequately predict how close a system is to voltage collapse, it must vary in a smooth, ideally linear, manner with respect to changes in the system (i.e. does not exhibit discontinuous changes in value for small system changes). The energy method has this characteristic since the contours in Figure 2-5 are fairly uniformly spaced. Third, the index should be relatively insensitive to the assumed path the system will take from the current operating point (for which the index is to be determined), and the point where the system is assumed to reach the feasible region boundary. This insensitivity is needed because this path is known beforehand only approximately at best. Strong dependence upon an assumed path can result in inaccurate rankings of various operating points. Consider the case where the current operating point is close to the boundary, but the assumed path is parallel to this boundary. This operating point would be ranked as quite secure, even though a slight variation in the actual path from the assumed path could result in loss of steady state stability. Since in the energy method the contours are parallel to the feasible boundary, this criteria is also met. Lastly, the computational time to calculate the index must be suitable for on-line use. The scalar energy difference is determined by simply solving for the current operating point (α^s, V^s) and for the unstable equilibrium (α^u, V^u), and then calculating the energy difference.

Therefore, at least for the 2 bus system, the energy difference provides a suitable indicator of proximity to voltage. Completing the example from the penultimate paragraph, Figure 2-6 shows how the energy difference varies as the load at bus 2 is increased so that the P/Q ratio remains constant at 2. The near linearity of the variation of the energy difference to change in load allows the sampling rate to be quite slow (approximately every 10% increment in load) and still yield excellent results.

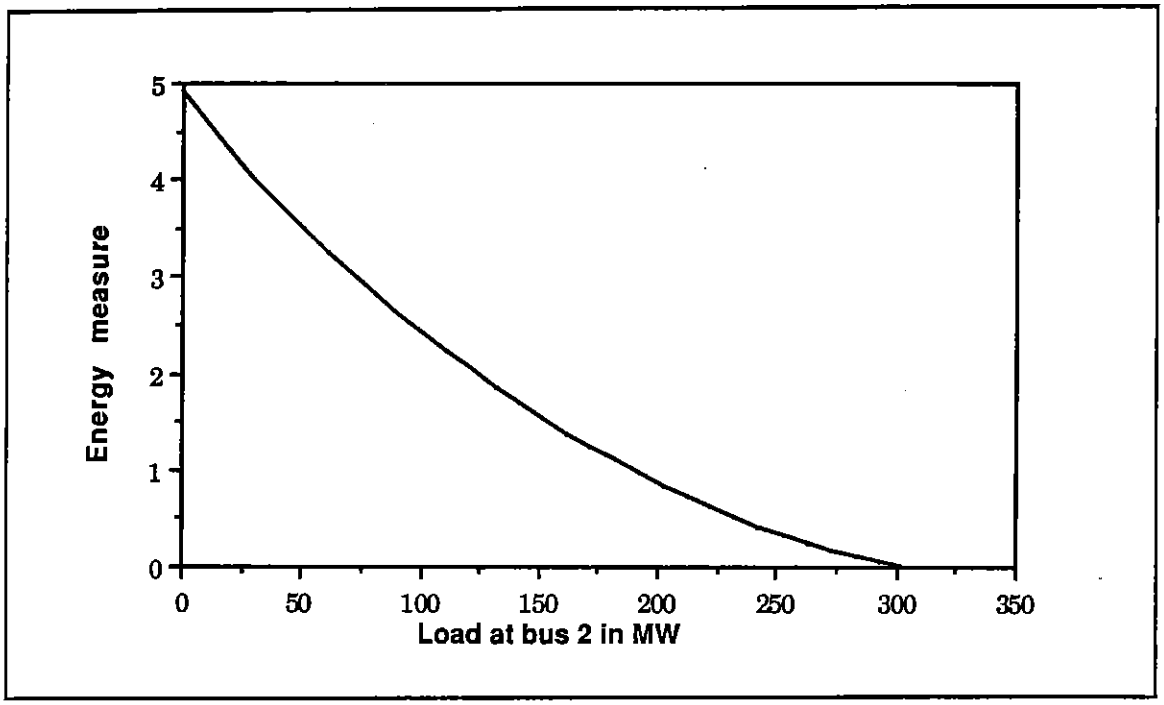

Figure 2-6 : Energy Measure versus Load Level for Two Bus System

For the lossless system previously studied it is possible to define an energy function which is truly a Lyapunov function. That is one in which energy is continuously nonincreasing along all trajectories, and the stable operating point is a local minimum of ϑ. This is no longer the case when losses are considered. Consider the realistic extension of (2-3) and (2-4) to include transmission line losses:

$$\begin{aligned} P_L + B_{12}V\sin(\alpha) + G_{12}V\cos(\alpha) + G_{22}V^2 &= f_{lossy}(\alpha,V) = 0 \\ Q_L - B_{22}V^2 - B_{12}V\cos(\alpha) + G_{12}V\sin(\alpha) &= g_{lossy}(\alpha,V) = 0 \end{aligned} \qquad (2\text{-}10)$$

Equation (2-6) could then be re-written, substituting f_{lossy} and g_{lossy} for f and g respectively. In trying to derive a Lyapunov function for this system of equations, we note

that Theorem 2.1 can no longer be applied to obtain a Lyapunov function because $\mathbf{A}^{-1}\partial \mathbf{f}(\mathbf{x})/\partial \mathbf{x}$ is no longer symmetric. In general for the case of a multimachine power system with losses, no global Lyapunov function has yet been found [25]. Instead the lossless Lyapunov function (2-8) is used to approximate the behavior of the system. Since losses are included in system differential equations, but not in ϑ, the derivative of ϑ along all trajectories

$$\dot{\vartheta}(\mathbf{x}) = \begin{bmatrix} M_g\omega & f(\alpha,V) & V^{-1}g(\alpha,V) \end{bmatrix} \mathbf{A} \begin{bmatrix} M_g\omega \\ f_{lossy}(\alpha,V) \\ V^{-1}g_{lossy}(\alpha,V) \end{bmatrix}$$

can no longer be guaranteed to be non-positive. Therefore ϑ is no longer formally a Lyapunov function; for the remainder of this proposal the term energy function will be used instead. Also since we are only interested in the value of ϑ at equilibrium points where $\omega = 0$ by definition, ϑ will no longer be written as a function of ω.

Another consequence of including losses in the system model is that $\vartheta(\alpha^s,V^s)$ no longer defines a local minimum of the ϑ function as defined in (2-8). A necessary condition for a local minimum of ϑ at (α^s,V^s) is that $\nabla\vartheta(\alpha^s,V^s) = \mathbf{0}$. However

$$\nabla\vartheta(\alpha^s,V^s) = \begin{bmatrix} f(\alpha^s,V^s) \\ V^{-1}g(\alpha^s,V^s) \end{bmatrix} = \begin{bmatrix} f_{lossy}(\alpha^s,V^s) \\ V^{-1}g_{lossy}(\alpha^s,V^s) \end{bmatrix} - \begin{bmatrix} G_{12}V\cos(\alpha) \\ V^{-1}G_{12}V\sin(\alpha) \end{bmatrix}$$

is no longer 0 since

$$\begin{bmatrix} f_{lossy}(\alpha^s,V^s) \\ g_{lossy}(\alpha^s,V^s) \end{bmatrix} = \mathbf{0}$$

by definition of an equilibrium point and $G_{12} \neq 0$ for a lossy system. This difficulty can be resolved at the stable operating point (α^s,V^s) by redefining f and g used in (2-7) to be

$$\begin{aligned} P_L + B_{12}V\sin(\alpha) + G_{12}V^s\cos(\alpha^s) + G_{22}(V^s)^2 &= f(\alpha,V) \\ Q_L - B_{22}V^2 - B_{12}V\cos(\alpha) + G_{12}V^s\sin(\alpha^s) &= g(\alpha,V) \end{aligned} \qquad (2\text{-}11)$$

Since the added terms in (2-11) are constants with respect to the variable of integration in (2-7), the vector function remains exactly integrable (i.e. no path dependence). With the addition of these constant offset terms, the gradient of the energy function at the stable equilibrium point is now identically zero. Note also that although the only explicit dependence of ϑ upon the system transfer conductances is through these offset terms, ϑ is implicitly dependent upon the transfer conductances since both of the limits of (2-7) reflect the influence of transfer conductances.

Using the redefined power balance equations (2-10), the revised energy function for the two bus system (2-8) is now

$$\begin{aligned} \vartheta(\omega,\alpha,V) := \; & \tfrac{1}{2}M_g\omega^2 - B_{12}V\cos(\alpha) + B_{12}V^s\cos(\alpha^s) - \tfrac{1}{2}B_{22}V^2 + \tfrac{1}{2}B_{22}(V^s)^2 \\ & + P_L(\alpha-\alpha^s) + Q_L\ln\left(\frac{V}{V^s}\right) + (G_{12}V^s\cos(\alpha^s) + G_{22}(V^s)^2)\;(\alpha-\alpha^s) \\ & + G_{12}V^s\sin(\alpha^s)\left(\frac{V}{V^s}\right) \end{aligned} \qquad (2\text{-}12)$$

As was done earlier, the revised energy function can be used to calculate an associated energy difference for any feasible load point (P,Q) in a system which includes transmission line losses. For example Figure 2-7 plots the energy contours of the system used for Figure 2-5 but with the addition of $G_{12} = -G_{22} = -5.0$. As was the case with the earlier figure, the energy contours are again both parallel to the feasible region boundary and fairly evenly spaced. Thus we can conclude that the energy approach provides a good index of proximity to voltage collapse in a two bus system, even when transmission line losses are included. In the next section the approach is extended to an arbitrary sized system.

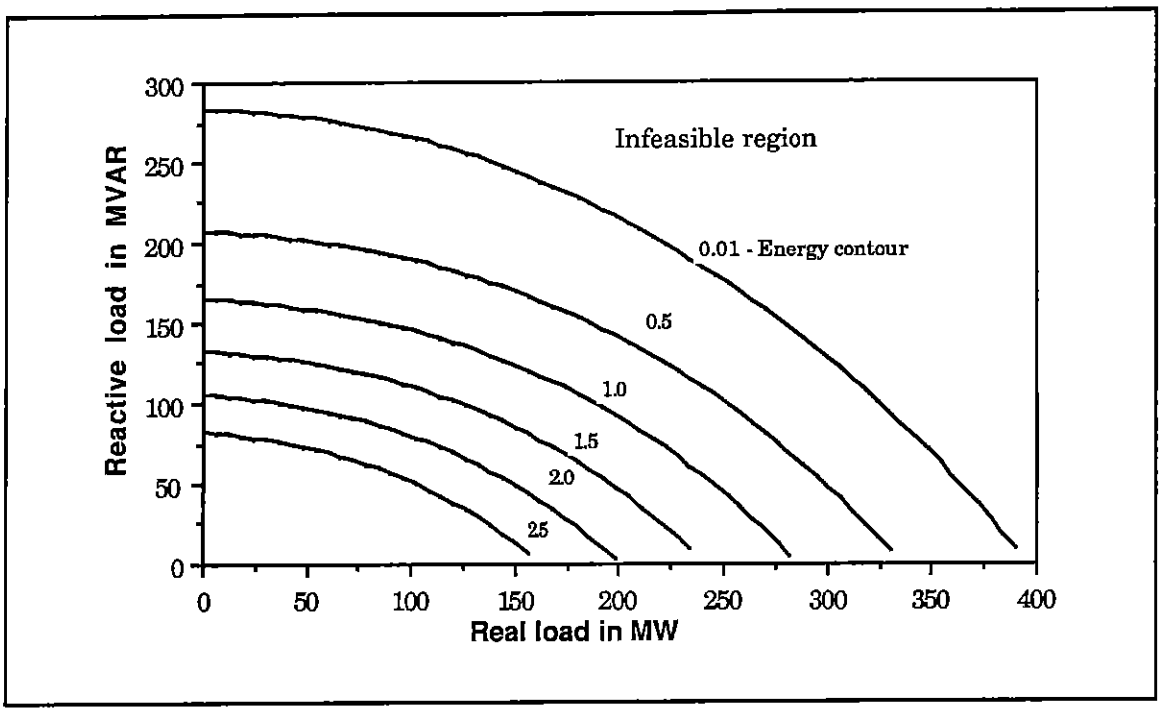

Figure 2-7 : Contours of Energy Function ϑ for Two Bus System with Losses

2.3 Application to Multiple Bus Power Systems

The two bus system model used in earlier sections is, of course, much too small to analyze all but the simplest of power systems. Today it is quite common for utilities to include several thousand buses in their power system models in order to accurately model the behavior of their electrical systems. In this section the application of the energy function method to system with more than two buses will be discussed.

Before delving into a discussion of the application of energy functions to multiple bus systems, it is important to clarify one point. For the two bus system the calculation of the high and low voltage solutions was straightforward. And there was at most one low voltage solution. However this, in general, is no longer the case for systems with more than two buses. Throughout this section we will make the assumption that both the high voltage solution, and the appropriate low voltage solutions of the powerflow equations are available. The former assumption is justified since the current operating point is normally either available on-line from the state estimator, or known in a planning study. The validity of the latter assumption will be touched upon in this section, but will be examined in much more detail in section 3.

Since we are only studying the properties of equilibrium points where $\omega \equiv 0$, we will focus on those terms in the differential equations of (2-5) remaining when $\omega = 0$ [26], i.e.

$$\dot{\alpha} = \mathbf{f}(\alpha, V) \tag{2-13a}$$

$$\varepsilon \dot{\mathbf{V}} = \mathbf{V}^{-1}\mathbf{g}(\alpha, V) \tag{2-13b}$$

where

ε = Constant positive diagonal matrix of parameters for singularly perturbed system model

The powerflow equations at each bus, f_i and g_i, can be written as

$$f_i(\alpha,\mathbf{V}) = P_i(V_i) - \sum_{j=1}^{n} B_{ij}|V_i||V_j|\sin(\alpha_i-\alpha_j) - \sum_{j=1}^{n} G_{ij}|V_i||V_j|\cos(\alpha_i-\alpha_j) \tag{2-14a}$$

$$g_i(\alpha,\mathbf{V}) = Q_i(V_i) + \sum_{j=1}^{n} B_{ij}|V_i||V_j|\cos(\alpha_i-\alpha_j) - \sum_{j=1}^{n} G_{ij}|V_i||V_j|\sin(\alpha_i-\alpha_j) \tag{2-14b}$$

where

B_{ij}, G_{ij} - Susceptance and conductance between buses i and j

V_i - Voltage magnitude at bus i

α_i - Voltage angle at bus i

$P_i(V_i)$ - Real power injection into the network at bus i (thus generation is positive while load is negative)

$Q_i(V_i)$ - Reactive power injection into the network at bus i

Thus (2-14) is simply an extension of (2-10) to an arbitrarily sized network. As is common in standard powerflow analysis, the voltage magnitude and angle are fixed at a single bus, known as the slack bus. For convenience bus n is chosen as the slack, with its angle set to 0. The voltage angle at bus i, α_i, is then defined with respect to the slack bus voltage angle. Normally the unknowns in the above equations are the voltage magnitudes and angles. They are solved for using the well-known Newton-Raphson iteration formula. Since equations (2-14) are sparse, spare matrix techniques can be used, resulting in quite reasonable computational solution times. Solution times on the order of a few seconds for a thousand bus model are common.

In a similar manner to what was done for the two bus case, an energy function ϑ can be developed using (2-7) when $P(V_i)$ is assumed to be independent of the voltage magnitude, and $Q(V_i)$ is an arbitrary polynomial or exponential function of bus voltage. In [27], it is shown that for a lossless system ϑ is formally a Lyapunov function. However the difficulty again arises that when the system model does contain losses (α^s,V^s) no longer defines a local minimum of ϑ. As was done for the two bus case, this difficulty is resolved at the stable operating point (α^s,V^s) by redefining **f** and **g** used in (2-7) as

$$f_i(\alpha,V) = P_i(V_i) - \sum_{j=1}^{n} B_{ij}|V_i||V_j|\sin(\alpha_i-\alpha_j) - \sum_{j=1}^{n} G_{ij}|V_i^s||V_j^s|\cos(\alpha_i^s-\alpha_j^s) \qquad (2\text{-}15a)$$

$$g_i(\alpha,V) = Q_i(V_i) + \sum_{j=1}^{n} B_{ij}|V_i||V_j|\cos(\alpha_i-\alpha_j) - \sum_{j=1}^{n} G_{ij}|V_i^s||V_j^s|\sin(\alpha_i^s-\alpha_j^s) \qquad (2\text{-}15b)$$

Since at (α^s,V^s) equations (2-15) are identical to (2-14), the gradient of the energy function at the stable equilibrium is now identically zero. The revised form of the energy function can then be expressed in closed form as [28]:

$$\vartheta(\mathbf{x}^u) = -\frac{1}{2}\sum_{i=1}^{n}\sum_{j=1}^{n} B_{ij}|V_i^u||V_j^u|\cos(\alpha_i^u-\alpha_j^u)$$

$$+\frac{1}{2}\sum_{i=1}^{n}\sum_{j=1}^{n} B_{ij}|V_i^s||V_j^s|\cos(\alpha_i^s-\alpha_j^s)$$

$$-\left(\sum_{i=1}^{n}\int_{V_i^s}^{V_i^u}\frac{Q_i(x)}{x}dx\right)-\mathbf{P}^T(\alpha^u-\alpha^s)$$

$$-\sum_{i=1}^{n}\left(\sum_{j=1}^{n} G_{ij}|V_i^s||V_j^s|\cos(\alpha_i^s-\alpha_j^s)(\alpha_i^u-\alpha_i^s)\right)$$

$$-\sum_{i=1}^{n}\left(V_i^s\right)^{-1}\sum_{j=1}^{n} G_{ij}|V_i^s||V_i^s|\sin(\alpha_i^s-\alpha_j^s)(V_i^u-V_i^s) \qquad (2\text{-}16)$$

In deriving (2-16), the integration in (2-7) was assumed to be between the stable equilibrium point (α^s,V^s) and an unstable equilibrium point (α^u,V^u). This was done since we are only concerned with the value of the energy function at the equilibrium points. For notational simplicity the dependence of $\vartheta(\mathbf{x}^u)$ upon the stable operating point $\mathbf{x}^s$ will not be explicitly identified.

The evaluation of the summation terms in (2-16) is straightforward. Again since the equations are sparse (i.e. many of the B_{ij} and G_{ij} terms are identically zero), the computational cost for calculating these sums is small (much less than that of a single powerflow solution).

For those buses with just load, the integral term can be quite easily evaluated when the reactive load is a polynomial or exponential function of bus voltage. For example, if the reactive load at bus i is constant, then the integral evaluates to

$$Q_i \ln\left(\frac{V_i^u}{V_i^s}\right) \qquad (2\text{-}17)$$

At the generator buses in the system generally the voltage magnitude is specified rather than the reactive output. The reactive injection at the generator bus then is assumed to vary in order to hold its bus voltage within a small tolerance of the given specified voltage (voltage setpoint). Exciter saturation is modeled by representing the reactive output of the generator as a function of terminal voltage, with saturation to specified upper and lower limits. With this model, the mathematical framework for treating voltage regulating generators is identical to that for voltage dependent reactive loads. A typical reactive power output versus terminal voltage characteristic is shown in Figure 2-8.

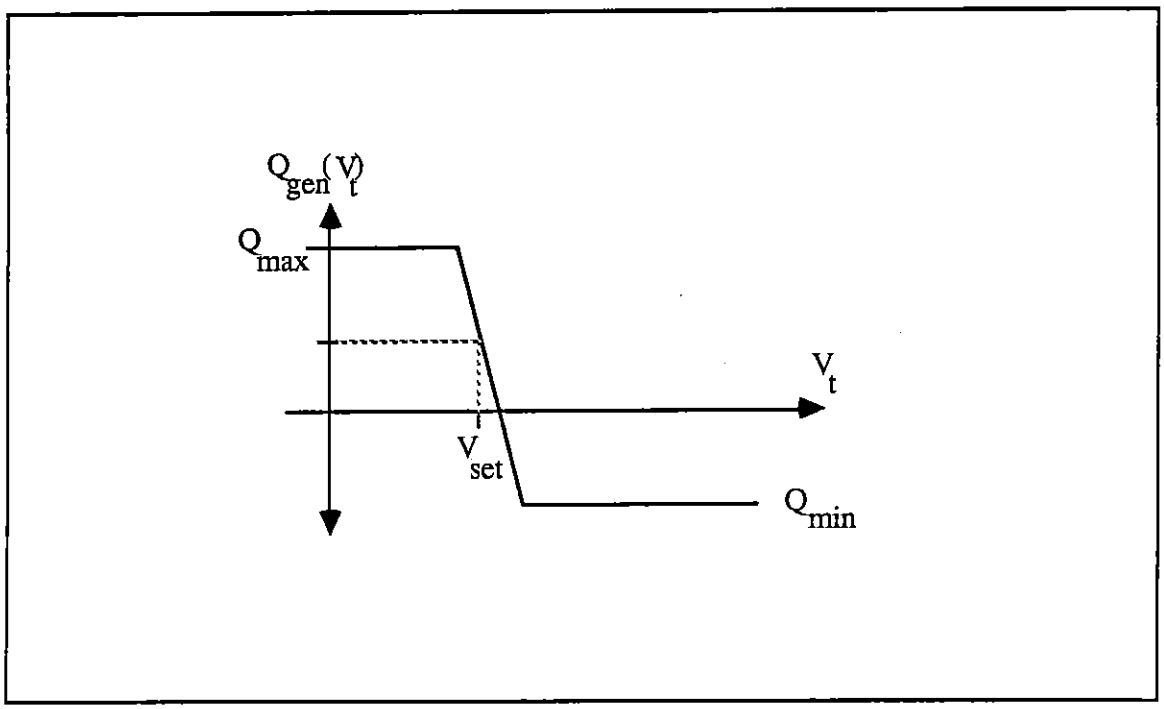

Figure 2-8 : Generator Reactive Output versus Terminal Voltage

If the reactive output of a given generator has not yet reached a limit at either the high or low voltage solution, then the deviation from this voltage setpoint is assumed to be very small. Thus the resulting integral term is negligible because the limits of integration are very close. However it is quite common for a number of generators to be pushed to their limits in the low voltage solution, while the generators are still regulating in the high voltage solution. In that case the integral term is well approximated by

$$Q_{lim(max)} * \ln\left(\frac{V_i^u}{V_i^s}\right) \qquad (2\text{-}18)$$

The rationale for this approximation is that along the integration path from the high solution V_i^s to the low solution V_i^u, the reactive output of the generator would rapidly saturate once the voltage had moved outside the small tolerance about its setpoint (Figure 2-8), and thus may be considered as a constant. Note that in this case (2-18) is the same as (2-17). This is to be expected since the generator bus is saturated along most of the path of integration and thus would behave as a constant reactive power source.

As the first step in complexity beyond the two bus system, consider the system shown in Figure 2-9. The system consists of a strong generator bus (an infinite or slack bus), with two separate load buses connected through lossy transmission lines. This system could be a rough representation of a large generating area supplying power to two separate urban centers. Since mathematically the system is simply equivalent to two independent two bus systems, it is clear that there are at most four powerflow solutions (both load buses at the high solution, one high and the other low, or both low) for this system.

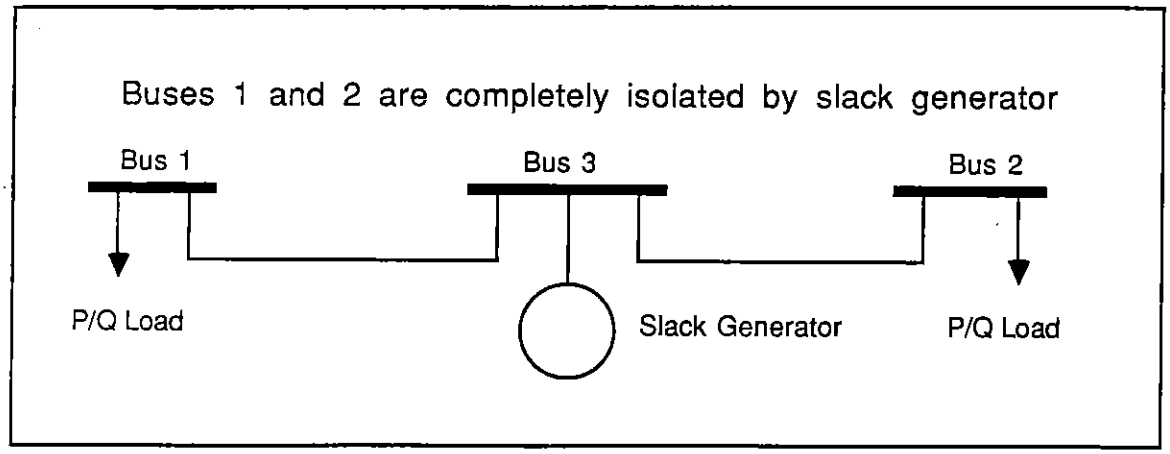

Figure 2-9 : One-line Diagram for Double Radial System

Then using (2-16) an energy difference between the operable high voltage solution and each of the low voltage solutions can be calculated. The independence of the two load buses allows for a straight forward interpretation of the energy measures. The two energy measures found using the solutions with one bus high and the other low can be used as a

proximity indicator to voltage collapse at each respective bus. Since the two loads are truly independent, the risk of voltage collapse at each bus is also independent. Hence a proximity indicator is needed for each. The energy measure calculated using the solution with both buses low is simply the sum of the other two indicators and thus could be interpreted to represent the risk of voltage collapse occurring simultaneously in both areas. The independence of the loads makes the probability of this occurring much less likely and therefore the proximity indicators of interest are the first two. Therefore the low voltage solutions of interest for this system are the first two. As was mentioned earlier, in this section we will assume that the appropriate solutions (and thus energy measures) are known.

The next logical extension of this system is to couple the two loads by adding a third line between them (Figure 2-10). Further assume that there is a generator at bus 1, which is initially off-line. The problem is then to determine the system's vulnerability to voltage collapse when it is characterized by a given load distribution (P_1, Q_1, P_2, Q_2). In this section the applicability of the energy method to providing such a measure is demonstrated.

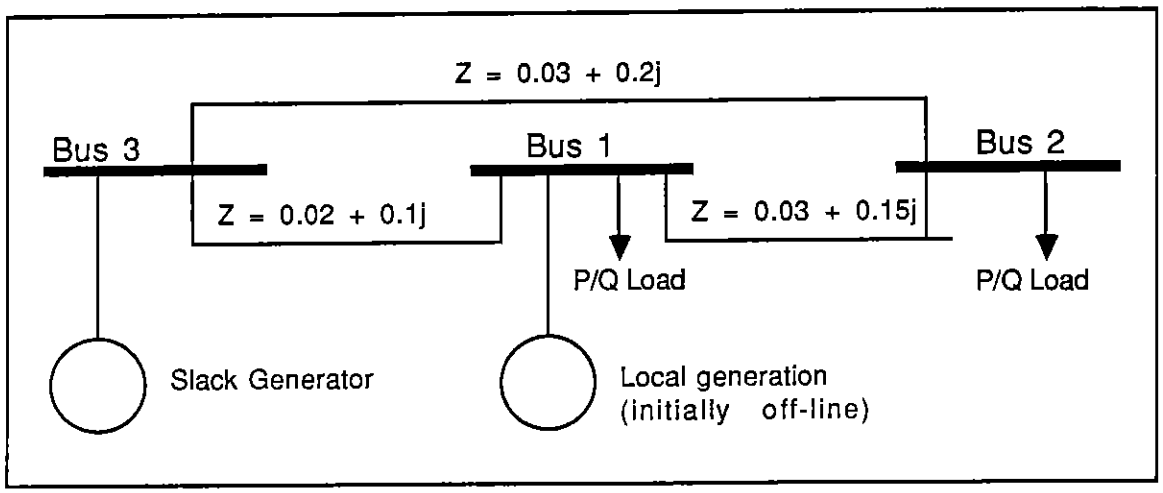

Figure 2-10 : One-line Diagram for Three Bus System

To determine the voltage vulnerability of this system using the energy approach it is first necessary that the appropriate low voltage solutions be calculated. Theoretically for an n bus power system there are believed to be at most 2^{n-1} solutions of the powerflow equations [29], [30]. However for a large system there are normally substantially fewer solutions, and only a small subset need to be determined. The technique used here is to

only consider those equilibrium points which are of type-one. A type-one equilibrium point is one in which a single eigenvalue of the linearized system about that equilibrium point is positive. Since the right-hand side of (2-13) consists of a positive diagonal matrix multiplying the powerflow equations, the number of positive eigenvalues can be determined from the Jacobian of the powerflow equations (2-14). The motivation for this approach comes from [31] where it is shown that the system always loses steady state stability by a saddle-node bifurcation between the stable equilibrium point (SEP) and a type-one UEP. The remainder of this chapter will justify this approach.

Returning again to the three bus system, with the assumption of constant load power factor (making Q_1 and Q_2 dependent variables), Figure 2-11 plots the energy contours of the feasible region in the (P_1,P_2) space. As was the case in Figure 2-5, the energy contours are parallel to the feasible region boundary and fairly evenly spaced. This again suggests that the energy measures provide a method of ranking the operating points (frozen equilibrium points) of the system.

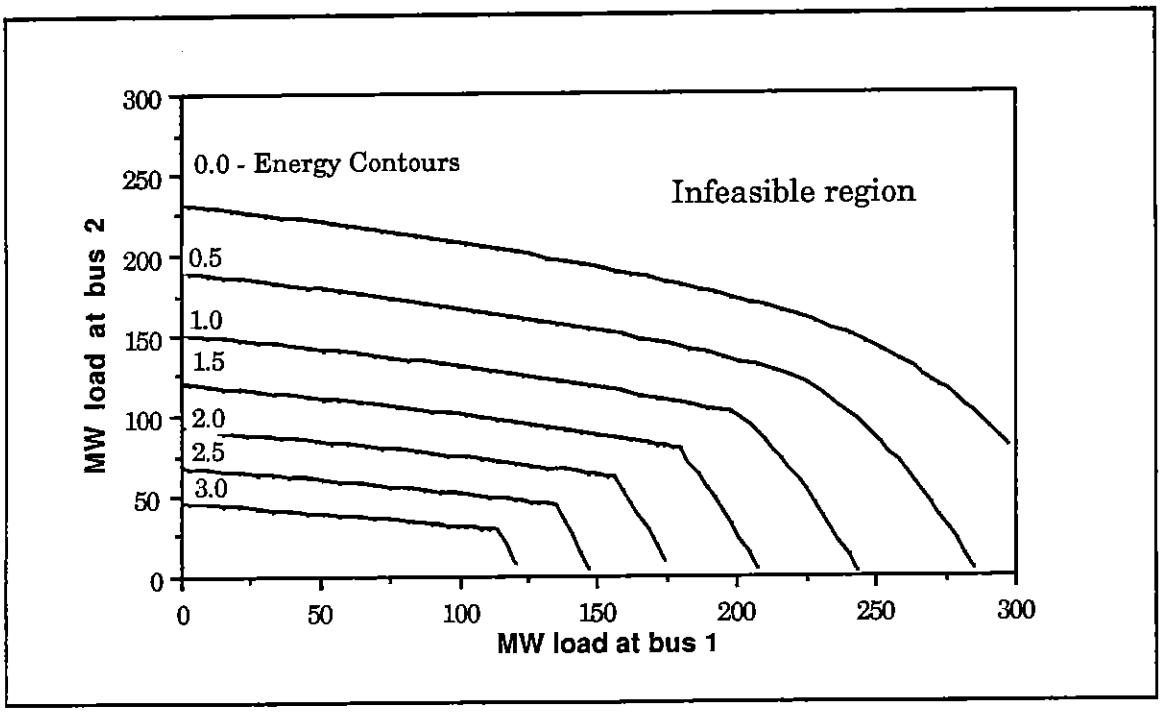

Figure 2-11 : Energy Contours for Three Bus System in P_1-P_2 Space

However the construction of Figure 2-11 was not as simple as for the two bus case. Since in a multi-bus power system there is often more than one low voltage solution, there are correspondingly often more than one energy measure. For a three bus system there are at

most a single SEP, two type-one UEPs, and a single UEP of type greater than one. This can be illustrated by plotting the voltage magnitudes at buses 1 and 2 as the system load is varied. For an initial load of 20 MW and 10 MVAR at each load bus, four solutions are possible. Figure 2-12 shows the solutions trajectories in the (V_2,V_3) space as the load at both buses is increased at the same rate, maintaining a constant power factor. The initial starting voltage points are labeled 1,2,3 and 4. Table 2-1 lists the four associated eigenvalues of each initial equilibrium point. As can be seen, solution one is an SEP, while solutions two and three are type-one UEPs, and solution four is a type-two UEP.

Table 2-1 - Solution Eigenvalues

Solution	Eigenvalues			
1	-19.9 + 3.9j	-19.9 - 3.9j	-6.6 + 1.1j	-6.6 - 1.1j
2	5.6	-0.5	-2.1	-4.3
3	-8.6	-6.5	4.0	-0.5
4	4.4	-0.5	-0.6	2.0

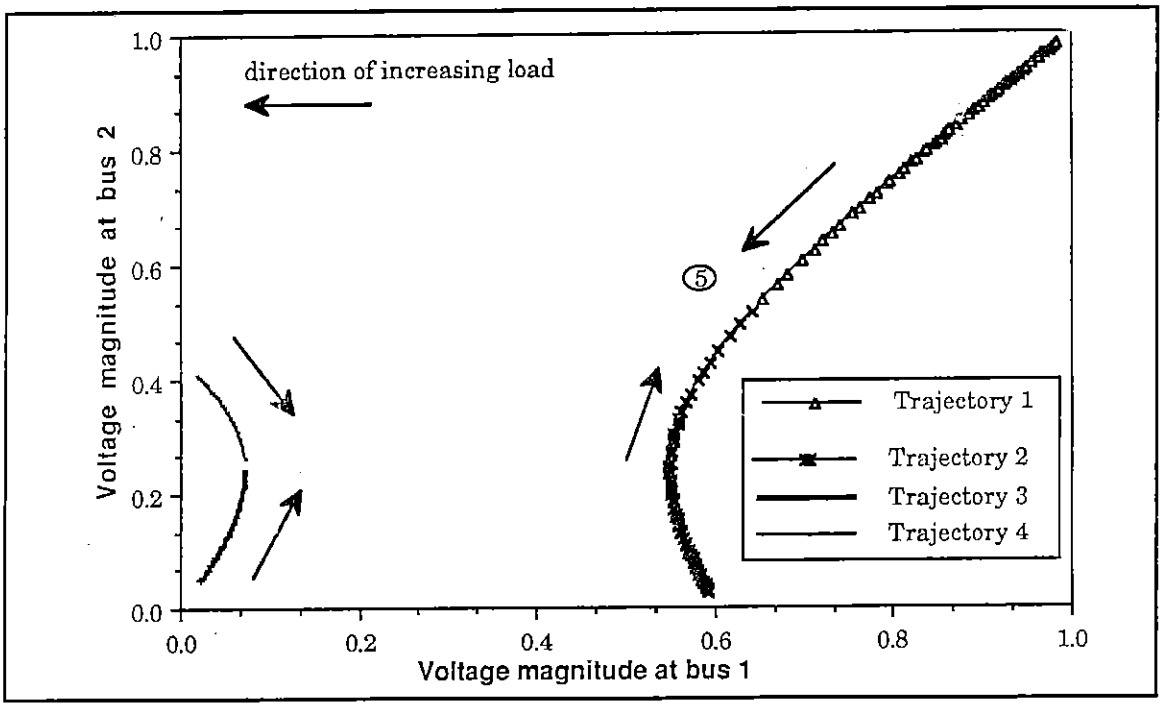

Figure 2-12: Variation in Voltage Magnitudes as Load is Increased

As the load is uniformly increased at buses 1 and 2, trajectory 1 moves downward to the left, indicating that the voltages at both buses are falling. This is reasonable behavior for a power system without voltage regulation. Eventually the voltage collapse point is reached (labeled point 5); at this critical point the Jacobian becomes singular and no further increase in load is possible. The power system has lost its stable equilibrium point; the deterministic dynamics of the system would then cause voltage collapse. Correspondingly, as the load is increased from its initial value, the solutions associated with the three low voltage solutions also move in the directions shown.

However at a load level significantly less than the load associated with the critical point, the solutions associated with trajectories 3 and 4 coalesce. For further increases in load these two solutions no longer exist. By the implicit function theorem [32] at the point where the two solutions merge the Jacobian must be singular. This occurs at a load of $P_1 = P_2 = 67$ MW. As the load is further increased, trajectory 2 continues upward, eventually meeting with trajectory 1 at point 5.

The number of powerflow solutions is dependent upon the loading of the system. In general as the loading of the system increases the number of solutions tends to decrease. As was demonstrated, these solutions vanish (and appear) in pairs. As the system approaches the voltage collapse critical point, the number of solutions goes to two. These two solutions eventually coalesce at the critical point. This occurs at a load of $P_1 = P_2 =$ 192 MW

An alternative way to show this voltage collapse scenario is Figure 2-13, which plots the energy difference between the stable solution and the three low voltage solutions versus load. Since there are initially three low voltage solutions, there are three energy measures. However as the loads increase, the upper two energy measures vanish when the solutions associated with trajectories 3 and 4 from above coalesce. Thereafter there is only a single energy measure for the system. As was assumed earlier, the energy measure for the non-type-one equilibrium is always larger than that of the type-one equilibriums. The final critical point is reached when the energy difference is zero.

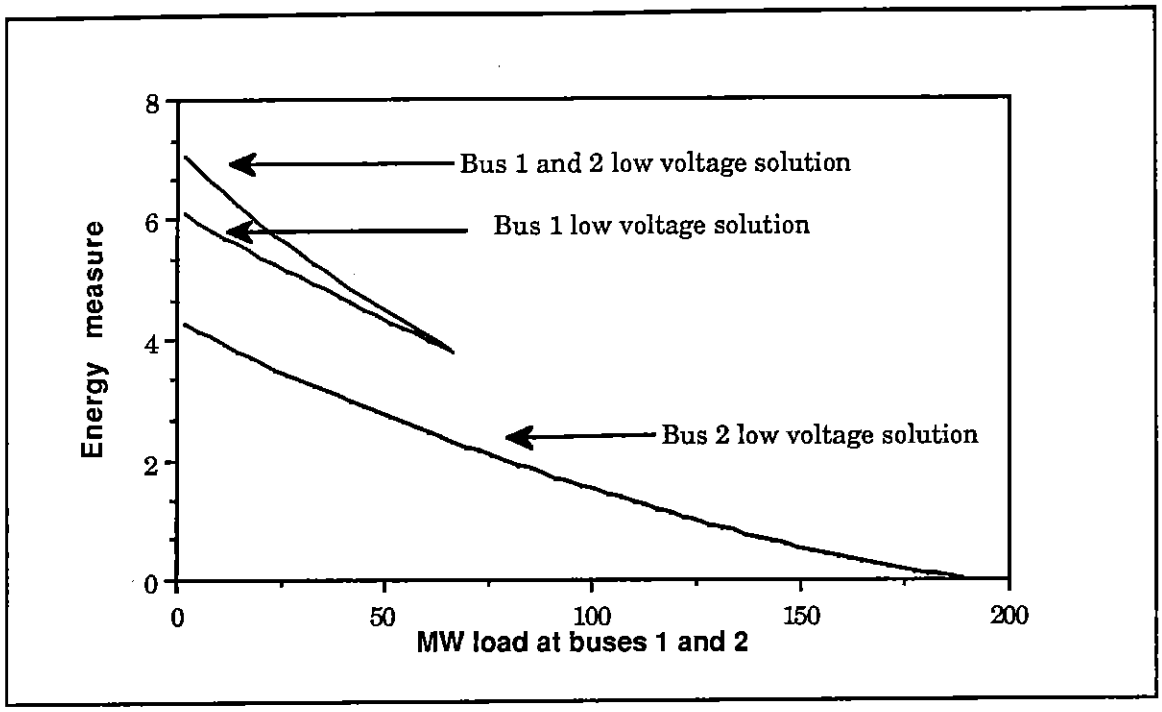

Figure 2-13 : Energy Measures for each Low Voltage Solution versus Load

The near linearity of the lower energy measure curve in the figure is due to the evenly spaced contours of Figure 2-11 parallel to the feasibility region boundary. To construct Figure 2-11 for those loadings with more than one associated energy difference, the lowest energy difference was chosen (which was always associated with a type-one equilibrium). When there was only a single low voltage solution (such as in the example above for loads greater than 67 MW) then that energy measure was used. Figure 2-14 shows the energy contours associated with each of the type-one equilibriums.

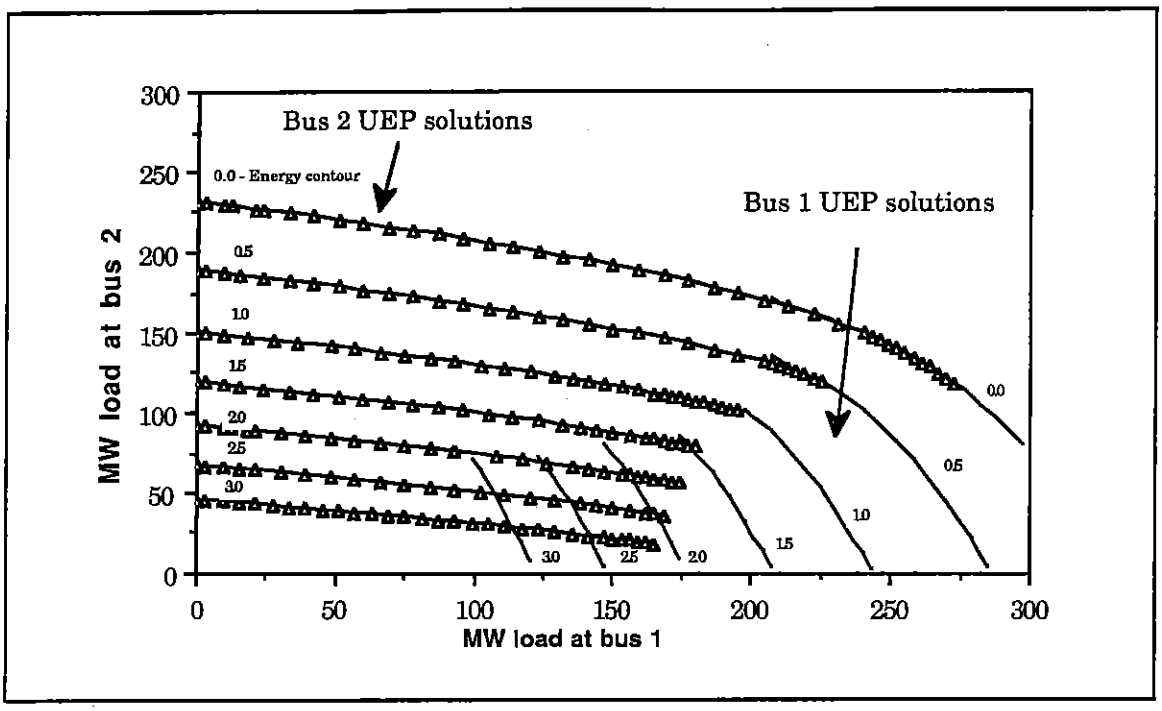

Figure 2-14 : Energy Contours for Each Type-one UEP

For those cases where there are more than a single type-one equilibrium, it is necessary to determine which of the possible energy measures are appropriate to use. This selection process can be illuminated by briefly discussing some properties of the low voltage solutions. At the point of bifurcation between the SEP $\mathbf{x}^0$ and a type-one UEP $\mathbf{x}^1$ (where $\mathbf{x}^0 = \mathbf{x}^1 = \mathbf{x}^*$), the SEP loses asymptotic stability with its Jacobian having a zero eigenvalue, $\lambda^1 = 0$. A slight perturbation in the state would then result in voltage collapse according to the deterministic dynamics of the system. In [31] it is shown that the initial direction of the voltage collapse is along the eigenvector $\mathbf{v}^1 = \mathbf{v}^*$ corresponding to the zero eigenvalue of the Jacobian at $\mathbf{x}^1$. The magnitudes of the individual components of $\mathbf{v}^1$ indicate how rapidly the voltage or angle at each individual bus will initially decline. Generally the magnitude of this initial voltage drop or angle slip is significant only at a subset of the system buses. This indicates that if voltage collapse were to occur via a bifurcation of $\mathbf{x}^0$ and $\mathbf{x}^1$, this subset would lead the rest of the system in collapse. Therefore while voltage collapse is characterized by loss of a steady state equilibrium for the entire system, its initial effects are normally apparent only at a subset of the system buses. Since these buses are usually electrically close to each other, the subset is referred to as an area. Notationally this area will be referred to as area($\mathbf{x}^1$). Thus we can talk about voltage collapse occurring in only an area of this system, while tacitly remembering that voltage instability is a system wide phenomenon.

Now assume that the system has not yet reached the point of bifurcation ($\mathbf{x}^0$ and $\mathbf{x}^1$ separate). Assuming that the system varies quasi-statically, whether $\mathbf{x}^0$ and $\mathbf{x}^1$ will coalesce depends upon the variation in $\mathbf{u}^{slow}(t)$. Since $\mathbf{x}^1$ is a type-one equilibrium, we can calculate the Jacobian's eigenvector $\mathbf{v}^1$ associated with the positive eigenvalue. Numerical testing indicates that the relative sizes of the components of $\mathbf{v}^1$ are fairly insensitive to the distance between $\mathbf{x}^0$ and $\mathbf{x}^1$ (recall that the energy difference is used as a distance function). Even while the two solutions are quite far apart, the components of $\mathbf{v}^1$ approximate how the system would collapse if the variation of $\mathbf{u}(t)$ was such that $\mathbf{x}^0$ and $\mathbf{x}^1$ eventually coalesced. Thus $\vartheta(\mathbf{x}^1)$ can be said to provide a proximity indicator to voltage collapse in area($\mathbf{x}^1$). When a system has more than a single type-one UEP, a separate energy difference could be calculated for each area($\mathbf{x}^i$). Each energy measure $\vartheta(\mathbf{x}^i)$ could be interpreted as a proximity indicator to voltage collapse occurring in area($\mathbf{x}^i$). Such an approach is needed since in an actual system there may be more than one area vulnerable to voltage collapse. As an example, Table 2-2 shows the variation in the components of the eigenvectors associated with each of the two type-one solutions for the three bus system for various loadings at buses 1 and 2.

Table 2-2 - Low Voltage Solution Eigenvector

Load - MW		Eigenvalues		Eigenvector (associated with positive eigenvalue)		Energy Measures	
P_1	P_2	$\mathbf{x}^1$	$\mathbf{x}^2$	$\mathbf{v}^1$	$\mathbf{v}^2$	$\vartheta(\mathbf{x}^1)$	$\vartheta(\mathbf{x}^2)$
180	180	-	-10.08	-	-0.16	-	0.10
			-0.58		-0.31		
			1.40		0.72		
			-0.58		0.60		
50	50	5.35	-8.32	-0.87	0.11	4.32	2.72
		-3.63	-6.28	-0.48	-0.12		
		-1.44	3.90	0.03	-0.87		
		-1.13	-1.15	-0.12	-0.50		
20	20	5.60	-8.61	-0.87	0.13	5.36	3.61
		-0.48	-6.46	-0.45	-0.10		
		-2.06	3.99	0.08	-0.88		
		-4.30	-0.48	-0.10	-0.47		

At the first load level in Table 2-2 of 180 MW, the system is heavily loaded and is close to voltage collapse. The first two rows in the eigenvector $\mathbf{v}^2$ are the components corresponding to the voltage angle and magnitude at bus 1, while the next two rows

correspond to the voltage angle and magnitude at bus 2. Based upon the relative size of these components, we can conclude that if voltage collapse were to occur through a bifurcation between this UEP solution and the SEP solution, the largest initial change in voltage would occur at bus 2. Area($\mathbf{x}^2$) could be defined as containing just bus 2. Then $\vartheta(\mathbf{x}^2)$ provides a proximity indicator to voltage collapse occurring at bus 2. Since there are no other solutions at this level of loading, we conclude that the vulnerable part of the system is bus 2. Referring to line parameters in Figure 2-10, this agrees with engineering judgement since bus 2 is more electrically distant than bus 1 from the point of voltage support (the slack bus). As the load is decreased to 50 and 20 MW, the largest components of $\mathbf{v}^2$ are still those associated with bus 2 and hence $\vartheta(\mathbf{x}^2)$ continues to provide a proximity indicator to voltage collapse occurring at bus 2.

For the lower load levels there is a second UEP $\mathbf{x}^1$. Since the largest components in its eigenvector $\mathbf{v}^1$ correspond to bus 1, we can likewise define area($\mathbf{x}^1$) as just containing bus 1. Then $\vartheta(\mathbf{x}^1)$ provides a proximity indicator to voltage collapse at bus 1. The components of the eigenvector are relatively insensitive to changes in the system loading. Again, because of the system structure and the equal loading at buses 1 and 2, the energy difference for voltage collapse at bus 2 is lower than the energy difference for voltage collapse at bus 1.

For the energy measure to provide an accurate indication of system proximity to voltage instability, it is important to include the effects of the various automatic controls of the system. Power systems normally contain a number of automatic controllers which attempt to maintain various system variables within predefined limits. Examples of such controls are excitation systems on generators, which regulate the generator terminal voltage; speed governors on generators, which maintain a constant system frequency; automatic generation control (AGC), which regulates the interchange of power between utilities; and load tap changing transformers (LTCs), which regulate the transformer voltage. These controllers also have limits on their control ranges. Once a control has reached its limit, it is no longer able to regulate its control variable. In normal operation most controls are within their regulation range. However, it is not uncommon (even in normal operation) for some controllers to be at their limits. The time constants on these controllers vary, but are typically on the order from under a second (generator excitation systems) to a few minutes (LTCs). Since the time scale of the voltage collapse problem under consideration here is on the order of tens of minutes to hours, it is important to include the effects of these controllers.

The applicable dynamic ranges of these controllers can be intrinsically included in the energy measure by assuming that they regulate both at the stable solution and at the low voltage solution. Limits on controller action must also be enforced at both solutions. The low voltage solution could be quite unrealistic if control limits are not enforced. This could cause the energy difference to provide an unreliable measure an proximity to voltage collapse (this is demonstrated in the example of the next paragraph).

The next example demonstrates the important property of the energy function; its ability to incorporate saturation of the generator excitation system. Using the three bus system from Figure 2-10, assume that the generator at bus 1 is now on-line but is only supplying reactive power for voltage support, holding its terminal voltage at 1.0 per unit. This system is a slightly more detailed representation of the type of system prone to voltage collapse. A large load local (buses 1 and 2) is being supplied mostly from distant generation (slack at bus 3). However some local voltage support is being provided (generator at bus 1). Voltage collapse will normally not occur until the local voltage support has saturated and is no longer able to maintain its setpoint voltage. Voltage regulation is modeled here by allowing the reactive output of the generator at bus 1 (Q_{G1}) to vary within some limits (Q_{G1}[max,min]) in order to hold its bus voltage constant. This is known as PV mode. When the reactive power has reached its maximum or minimum, the generator's exciter is assumed to have saturated, and the generator's reactive output is subsequently held constant. This is known as PQ mode.

One would expect that the more maximum reactive power the generator can provide, the greater the load which can be tolerated, and the subsequently the more secure the system for any particular load. Figure 2-15 shows that this is indeed the case. Using the voltage collapse scenario from the previous example (bus 1 load = bus 2 load), the lowest curve shows how the energy measure would vary if there was zero output from G_1 (in other words the generator is off-line) and is therefore a repeat of the lower curve from Figure 2-13. The next three curves show how the energy function varies as the maximum var output of generator 1 is increased in increments of 100 MVAR. During the sequence of powerflow/energy calculations, the voltage at bus 1 was held at 1.0 per unit as load ramped up until Q_{G1} reached its limit. Thereafter the var output was held at its maximum, with the generator switching from PV to PQ. Table 2-3 shows how the generator reactive output and energy difference vary as the maximum reactive limit was changed.

Table 2-3 - Generator Reactive Limits

Load MW		Bus 1 MVAR Generation .			
bus1	bus2	SEP	UEP	Max MVAR	Energy
150	150	0	0	0	0.55
150	150	100	100	100	0.92
150	150	192	200	200	1.26
150	150	192	300	300	1.54

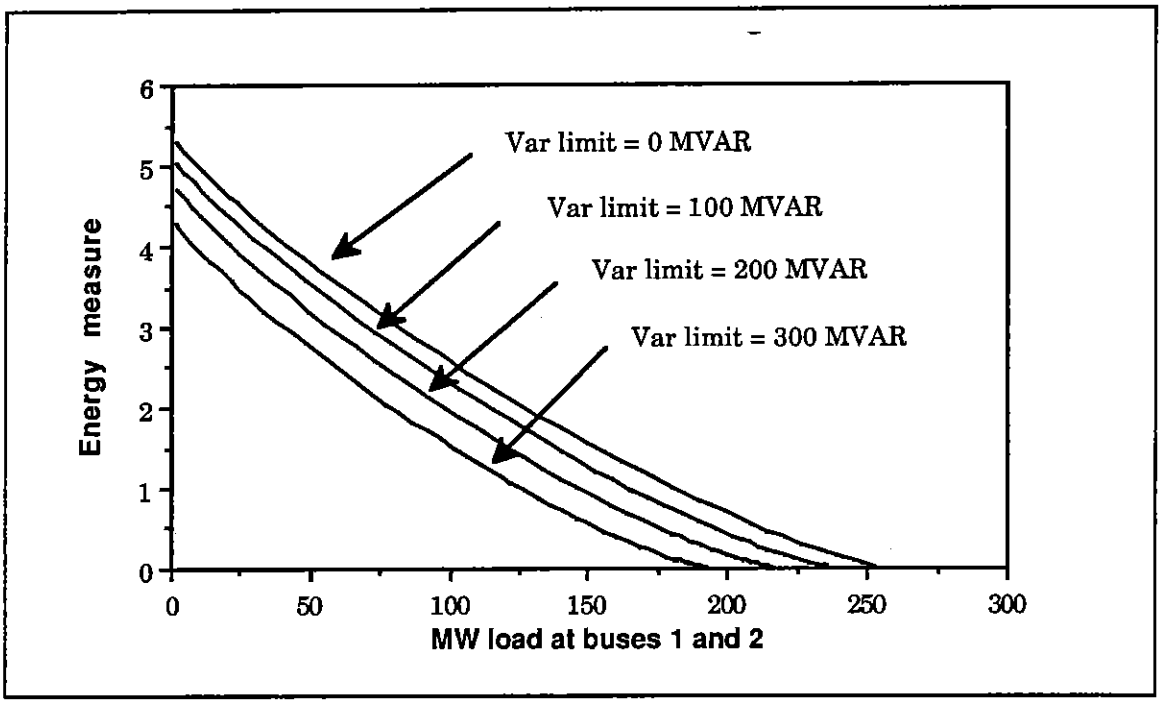

Figure 2-15 : Effect of Generator MVAR Limits on Energy Measure

As would be desired, the energy measure increases as the maximum reactive limit of the unit is increased. Note that the limits on available var support are taken into account even when the current system operating point does not push generators to these limits. This property is important since one would like an accurate determination of system voltage security before local generators have saturated (at which point it may be too late to prevent voltage collapse).

Intuitively, the ability of the energy measure to incorporate reactive limits of non-saturated units is because the low voltage solution tends to push the var source to its limit. The var

limits thus reduce the height of the potential energy boundary that the system must cross to experience collapse. If the generator regulation status at the low voltage solution was incorrectly always assumed to be that of the high voltage solution (PV or PQ), the energy curve could exhibit discontinuities. This is shown in Figure 2-16 for the case with var limits of ± 300 MVAR. The reason for the discontinuities is apparent from a plot of low voltage generator reactive output vs system load (Figure 2-17). As Figure 2-15 indicates, such discontinuities are eliminated when var limits are enforced independently at both solutions.

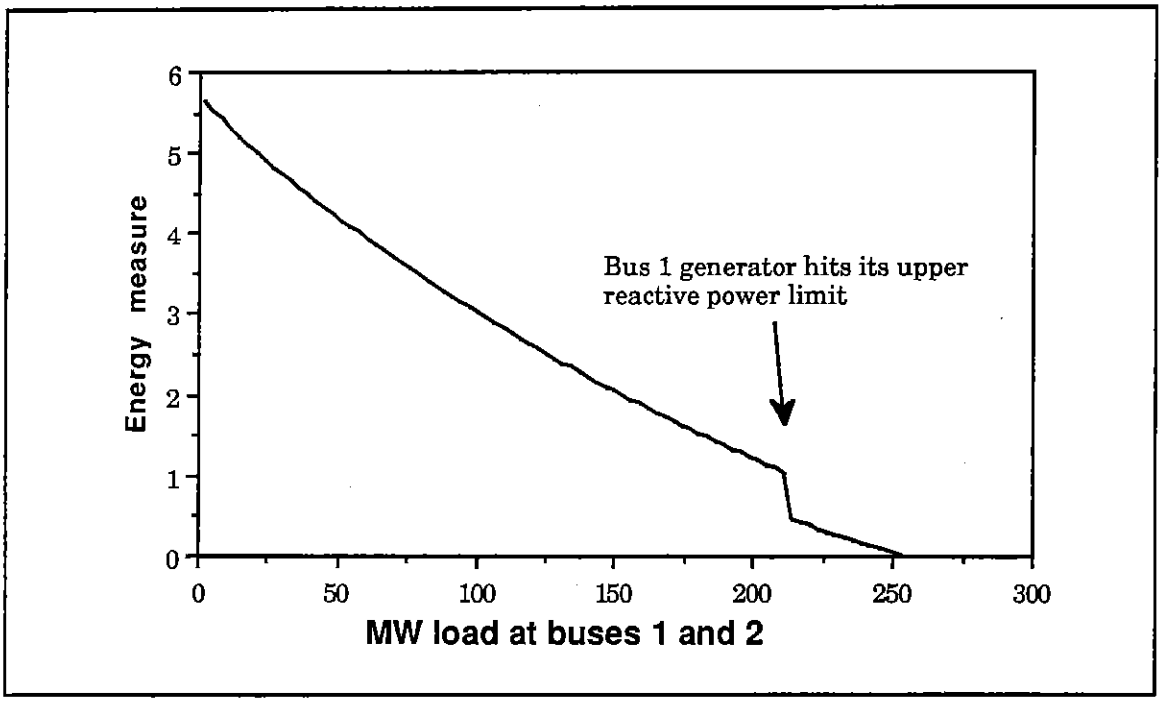

Figure 2-16 : Energy Measure versus Load when Var Limits are not Enforced at Low Voltage Solution

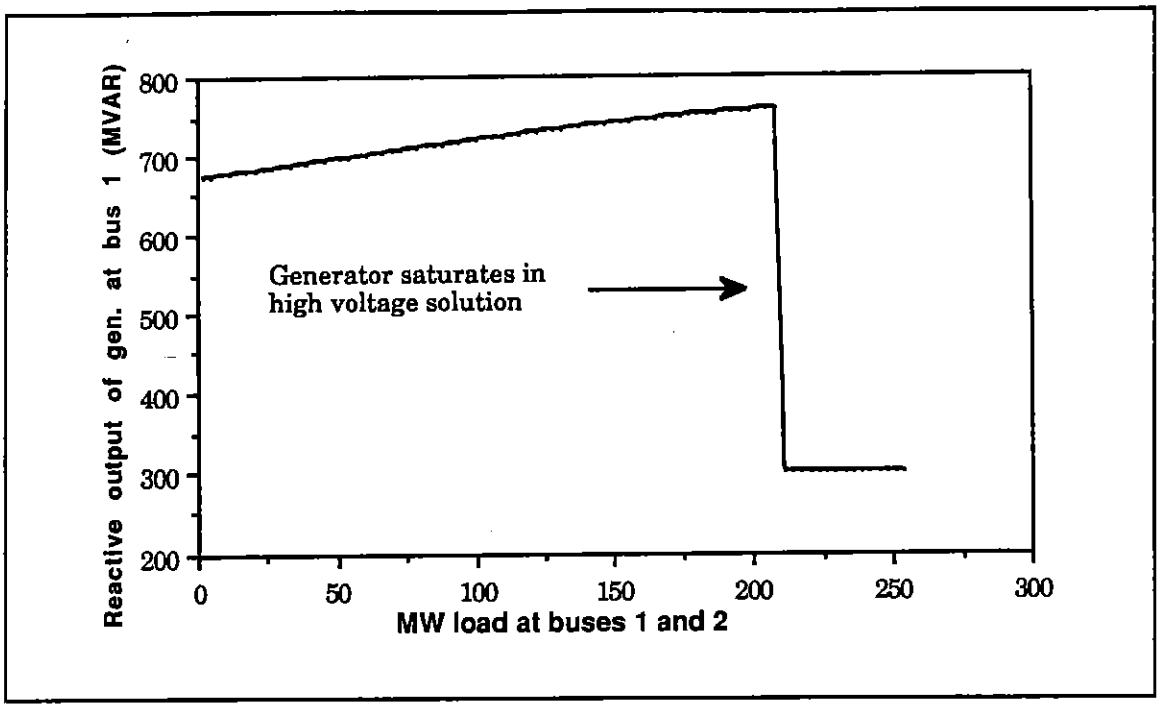

Figure 2-17 : Generator Reactive Output versus Load for Low Voltage Solution

The energy method can also be applied to larger systems. As with the case of the three bus system, energy differences are calculated between the stable solution and the appropriate type-one UEP solutions. These energy differences then provide a measure of how close the system is to voltage instability. The following example illustrates the usefulness of the energy method on a larger system. The New England 30 Bus system (NE30) used in [33] and [34] was chosen since it is the standard system for testing voltage instability proximity measures. The following voltage collapse scenario shows that the variation in the energy difference is proportional to changes in the system operating point. The reactive load at bus 11 (Q_{11}) was increased until voltage collapse occurred, while keeping all other loads and generator MW outputs fixed. This is scenario number 1 from [33]. The two curves in Figure 2-18 represent the energy differences between two type-one UEPs and the stable solution as the reactive load at bus 11 is increased (until voltage collapse occurs). The upper left-hand curve corresponds to the energy difference associated with voltage collapse in the area centered on bus 12. The lower right-hand curve corresponds to the energy difference associated with voltage collapse in the area centered on bus 11. For low load levels only the bus 12 low voltage solution exists; for load levels at Q_{11} between about 450 and 550 MVARs both solutions exist; while for high loads only the bus 11 low voltage solution exists. Because only the reactive load at bus 11 is being increased in this scenario,

it is not unsurprising that voltage collapse should ultimately be characterized by a bifurcation between the low voltage solution associated with bus 11 and the stable solution.

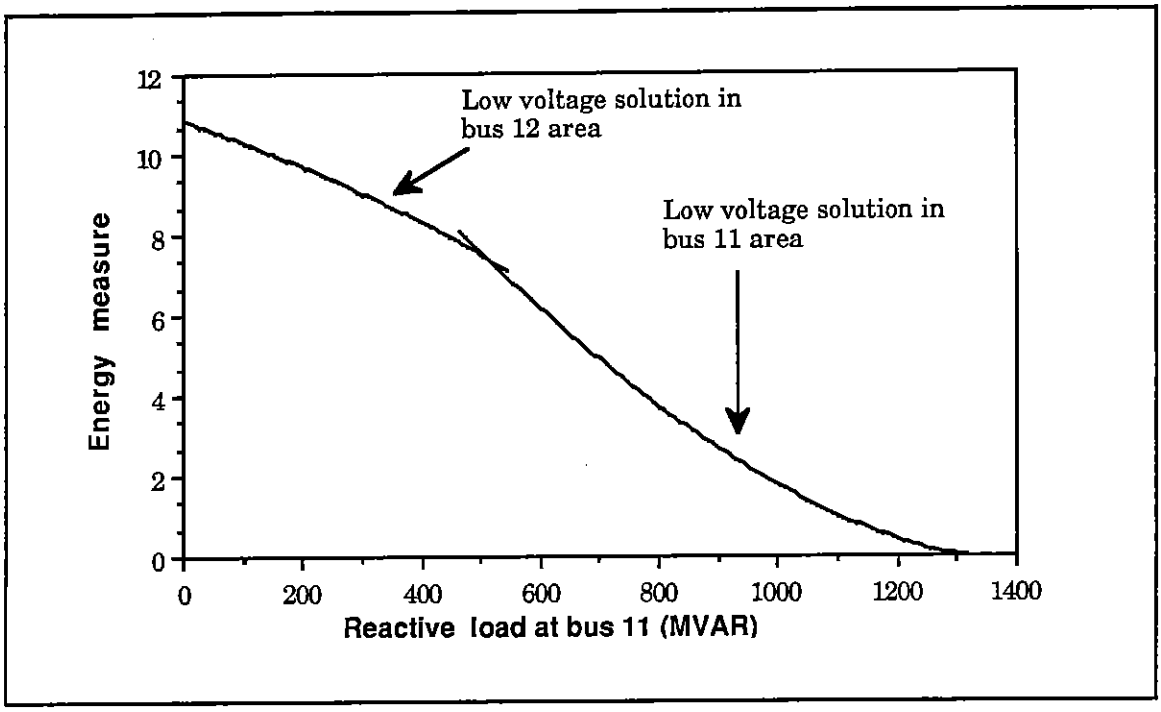

Figure 2-18 : Energy Measure Curve for 30 Bus System

As was the case with the smaller systems, the proximity indicator is defined as the minimum of the energy measures. Note that the minimum values varies in a proportional (approximately linear) manner to the variation in the system operating point. Figure 2-18 may be compared to the plots of other proximity measures in [34] for the same voltage collapse scenario.

By monitoring the variation in the energy measure over time, the system operator would have a good idea of when corrective control actions are needed to increase system voltage security. For example again assume that all loads are fixed, except for the reactive load at bus 11; Figure 2-19 plots the variation in Q_{11} as a function of time. Figure 2-20 plots the corresponding variation in the energy measure. Since the system loses its stable operating point anytime the energy difference is zero, a number of criteria could be used to notify the operator when voltage collapse is impending. One simple notification criterion would be anytime the minimum energy difference falls below a given tolerance. If the tolerance was $\vartheta = 0.5$, this would occur for the system in Figure 2-20 at hour 14. Another criterion would be anytime the value of ϑ divided by the decrease in the energy with respect to time

was less than a time tolerance. That is, if the energy continues to decrease at the present rate, voltage collapse would occur in less than the tolerance amount of time. By setting this tolerance to a large enough value, the operator should have time to take correct action to avert a voltage collapse. A discussion of how the energy method could be applied to enhance system security is provided in [28].

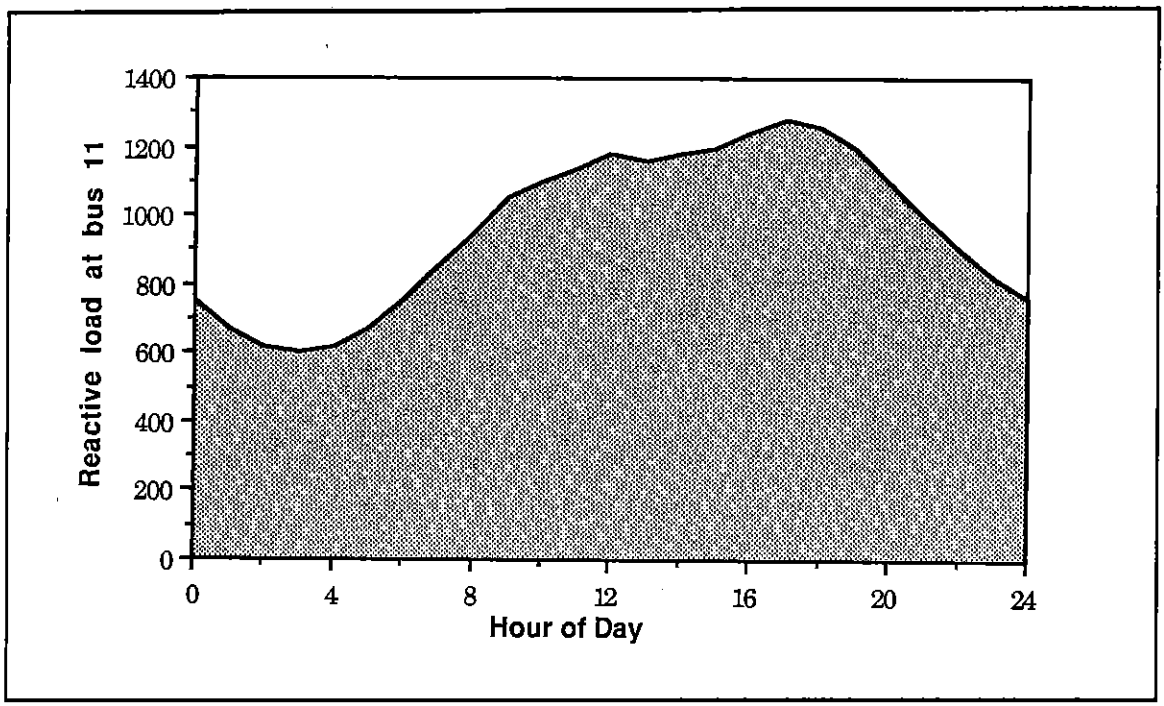

Figure 2-19 : Daily Variation in Reactive Load at Bus 11

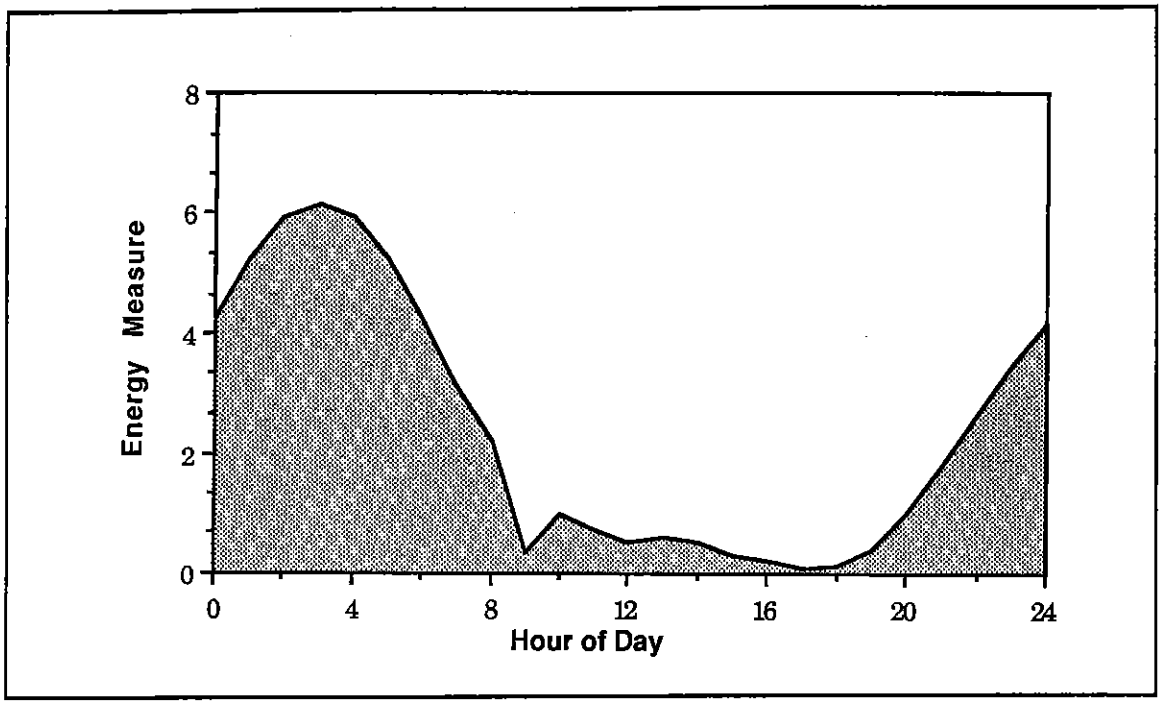

Figure 2-20 : Daily Variation in Energy Measure

CHAPTER 3 - LOW VOLTAGE POWERFLOW SOLUTIONS

In this chapter the properties of, and solution techniques for low voltage solutions are discussed. As was seen in chapter 2, in order to apply energy methods to the voltage collapse problem, it is crucial that the appropriate low voltage solutions can be found with reasonable computational effort. First the properties of the two powerflow solutions for the two bus system are briefly discussed. Then the properties of low voltage solutions of multiple bus system are discussed. Finally algorithms are proposed for finding the appropriate low voltage solutions of large systems.

In Chapter 2 the powerflow equations (2-14) were written with the complex voltages expressed in polar form. This method was chosen in order to exploit the physical meaning of bus voltage magnitude and angle in the derivation and use of the energy function. However, these equations could also be rewritten with the voltages expressed in rectangular form of $V_i = e_i + jf_i$. The equivalents to (2-14) are then

$$f_i(\mathbf{e},\mathbf{f}) = P_i - \sum_{j=1}^{n} \{e_i (e_j G_{ij} - f_j B_{ij}) + f_i (f_j G_{ij} + f_j B_{ij})\} \qquad (3\text{-}1a)$$

$$g_i(\mathbf{e},\mathbf{f}) = Q_i - \sum_{j=1}^{n} \{f_i (e_j G_{ij} - f_j B_{ij}) - e_i (f_j G_{ij} + e_j B_{ij})\} \qquad (3\text{-}1b)$$

Experience has shown that the rectangular form of the powerflow equations is the preferred representation for computing the low voltage solutions. Therefore the rectangular representation will be primarily used in this chapter.

3.1 Powerflow Solutions of Two Bus System

For the 2 bus system shown in Figure 2-1, where the slack voltage is assumed to be $e_1 + j f_1$, (3-1) simplifies to the real and reactive mismatch equations at the load bus:

$$P_L = G_{22}(e_2^2 + f_2^2) + A_2 e_2 + B_2 f_2 \tag{3-2a}$$

$$Q_L = B_{22}(e_2^2 + f_2^2) + B_2 e_2 - A_2 f_2 \tag{3-2b}$$

where

e_2, f_2 = Real and imaginary load bus voltages
A_2 = $e_1 G_{12} - f_1 B_{12}$
B_2 = $e_1 B_{12} + f_1 G_{12}$

It is then possible to solve directly for e_2 and f_2 [24]

$$e_2 = \frac{-b \pm \sqrt{(b^2 - 4ac)}}{(2a)} \tag{3-3}$$
$$f_2 = \alpha e_2 + \beta$$

where

$$\alpha = \frac{G_{22}B_2 - B_{22}A_2}{B_{22}B_2 + G_{22}A_2}$$

$$\beta = \frac{G_{22}Q_L + B_{22}P_L}{B_{22}B_2 + G_{22}A_2}$$

$a = G_{22}(1+\alpha^2)$
$b = 2\alpha\beta G_{22} + A_2 + B_2$
$c = G_{22}b^2 + B_2\beta + P_L$

Thus we conclude that (3-2) has at most two solutions. If $b^2 > 4ac$ then there are two solutions (recall that each solution can be thought of as a point of intersection of the two

power balance constraints from [3-2]). If $b^2 = 4ac$ then there is only a single solution (the two power balance constraints become tangent). At this point the powerflow Jacobian is singular. If $b^2 < 4ac$ then the system of equations has no solution (the power balance constraints never intersect).

3.2 Powerflow Solutions of Multi-bus System

The determination of the appropriate low voltage solutions is of crucial importance in applying the energy function method to the voltage instability problem. As was mentioned earlier, for an n+1 bus power system, there are believed to be at most 2^n separate powerflow solutions. If it was necessary to attempt to find all these solutions, the energy method would be computationally intractable for all but the smallest systems. In this section the properties of, and solution algorithms for the low voltage solutions of multi-bus systems will be examined.

3.2.1 Simplified Solution Method

The earliest algorithm to calculate all of the low voltage solutions of a system was presented in [24]. The algorithm presented can be summarized as follows:

1. Obtain the stable operating point powerflow solution $\mathbf{V}^s$.

2. Using the quadratic algorithm from section 3.1, calculate the low voltage "solution" for each load bus assuming that the voltages at all the other buses are fixed. This calculation is not performed at buses which have voltage regulation (PV buses) or at the system slack. Denote this voltage as V_i^u.

3. Select either $\mathbf{V}_i^s$ or $\mathbf{V}_i^u$ as initial voltage guesses for the rectangular Newton-Raphson algorithm. Form all of the $2^{(n-m)} - 1$ possible combinations of initial voltage guesses (where m is the number of PV buses).

4. Compute powerflow solutions using the rectangular Newton-Raphson algorithm for each of the $2^{(n-m)} - 1$ initial voltage guess permutations. The

optimal multiplier method [35] is used to prevent the powerflow from diverging or oscillating.

Using this exhaustive search technique, the authors were able to demonstrate that the number of actual solutions in most systems was substantially less than the maximum number. For example for a lightly loaded eleven bus system with two PV buses, out of the 255 possible solutions only 57 existed. As the loading on the system increased the number of solutions decreased, so that there was only a single low voltage solution immediately before loss of the stable equilibrium solution. However in order to find this small number of solutions, it is still necessary to test the $2^{(n-m)}$ initial guesses if the above algorithm is used.

Fortunately a "simplified" algorithm was also presented which substantially decreased the number of necessary initial guesses. The simplified algorithm is essentially the same as the exhaustive method, except that rather than forming all of the $2^{(n-m)} - 1$ initial voltage guess combinations, only the n-m combinations corresponding to using V_i^u at a single bus are calculated. Using this method only 8 solutions had to be calculated for the sample system. Again, the number of simplified solutions which actually exist depends upon the loading of the system. For a more heavily loaded system, such as the New England 30 bus (with Q_{11} = 1200 MVAR), there are only 3 simplified method solutions (corresponding to low initial voltage guesses at buses 1, 11 and 28).

Testing suggests that the solutions obtained by the simplified method correspond to the type-one UEPs mentioned in the previous chapter. Recall that loss of voltage stability, if it were to occur, would take place by a bifurcation between the SEP and a type-one UEP. Therefore it is only necessary to calculate an energy difference between the SEP and the solutions obtained by the simplified method. Additionally, the voltage collapse areas defined in Chapter 2 are centered on the bus with the low initial voltage guess. For example in Table 2-2, $\mathbf{x}^1$ was found using a low initial guess at bus 1, while $\mathbf{x}^2$ was found with a low initial guess at bus 2.

3.2.2 Improvements to Simplified Method

In general not all n simplified low voltage solutions exist. However, it would still be computationally prohibitive (for a large system) to have to perform n powerflows in order to determine which of the solutions exist and are pertinent. In this section various enhancements to the simplified method are discussed.

Let $\mathbf{x}^i \in R^{2n}$ denote the simplified low voltage solution calculated with a low initial voltage guess at bus i. Recall that the voltage vector $\mathbf{x}$ can be represented in either rectangular or polar coordinates. When the rectangular form of the powerflow equations is used, $\mathbf{x}$ is partitioned as $\mathbf{x} = [e_1, f_1, e_2, f_2, \ldots, e_n, f_n]$; when the polar form of the equations is used, $\mathbf{x}$ is partitioned as $\mathbf{x} = [\alpha_1, V_1, \alpha_2, V_2, \ldots, \alpha_n, V_n]$. Since each solution $\mathbf{x}^i$ is hypothesized to correspond to a type-one UEP, we can calculate the eigenvector associated with the positive eigenvalue of the Jacobian of (2-15) (polar representation). From the discussion of Chapter 2, it was seen that the magnitude of the eigenvector components define an area denoted area($\mathbf{x}^i$). The energy measure $\vartheta(\mathbf{x}^i)$ is then interpreted as a proximity indicator to voltage collapse occurring in area($\mathbf{x}^i$). Experimentation indicates that if solution $\mathbf{x}^i$ exists, bus i is within area($\mathbf{x}^i$) and often has the largest corresponding eigenvector components.

For example consider the voltage collapse scenario shown in Figure 2-18. For high values of load at bus 11, the energy difference was found by initializing the powerflow with the voltage at bus 11 low. Hence we would expect the eigenvector associated with the positive eigenvalue of the low voltage Jacobian should have its largest components at bus 11. The eigenvector components are shown in Figure 3-1 for a reactive load at bus 11 of 1300 MVAR. The largest component was at bus 11 (the eigenvector was normalized so that the largest component was 1.0), with the next largest components at the first neighbors of bus 11 (buses 6, 10, and 12). Figure 3-2 shows the eigenvector components when the load is decreased to 800 MVAR. Again the largest component was at bus 11, with significant other components at its first and second neighbors. As the load at bus 11 is decreased, eventually the low voltage solution found by initializing with bus 11 disappears. However a new solution, found by initializing the powerflow with bus 12 low, appears. Figure 3-3 shows the components for this solution's positive eigenvalue eigenvector when the load at bus 11 is 400 MVAR. As would be expected, the largest component is now at bus 12. It should be emphasized that it is not necessary to calculate the Jacobian eigenvectors in order to calculate the low voltage solutions. The eigenvectors were only shown here to

demonstrate that the simplified solution $\mathbf{x}^i$ can be used to determine the risk of voltage collapse initiating in the area roughly centered around bus i.

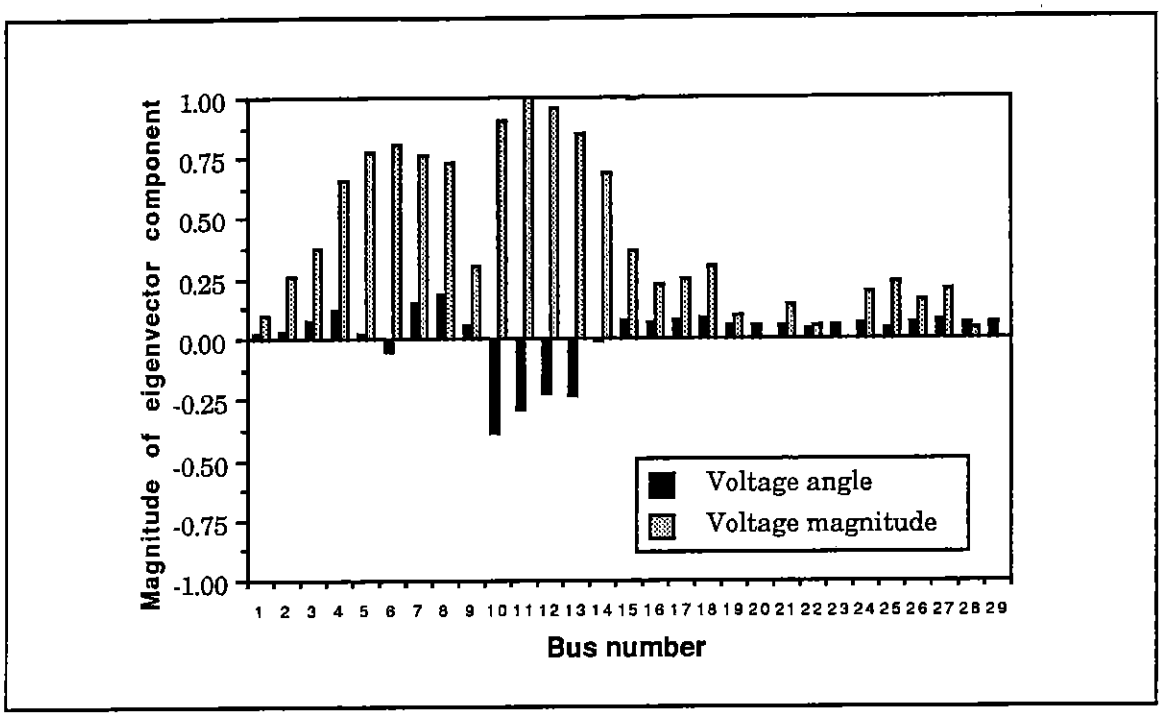

Figure 3-1 : Components of eigenvector associated with positive eigenvalue of UEP solution Jacobian when reactive load at bus 11 = 1300 MVAR

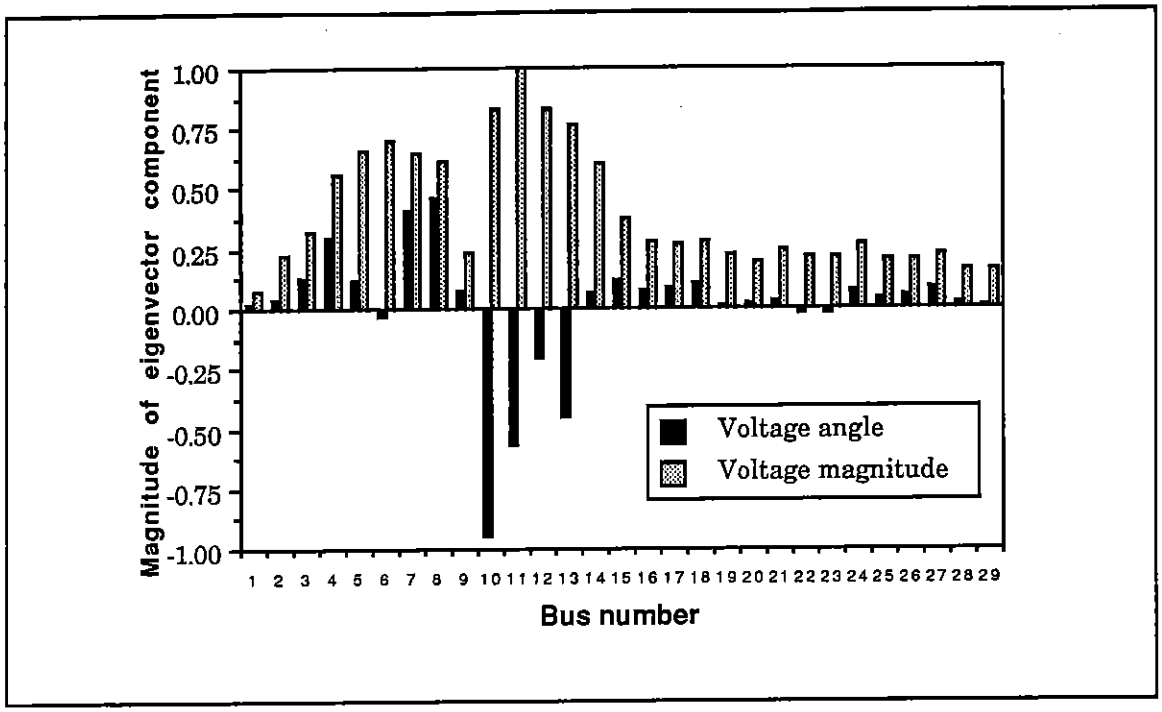

Figure 3-2 : Components of eigenvector associated with positive eigenvalue of UEP solution Jacobian when reactive load at bus 11 = 800 MVAR

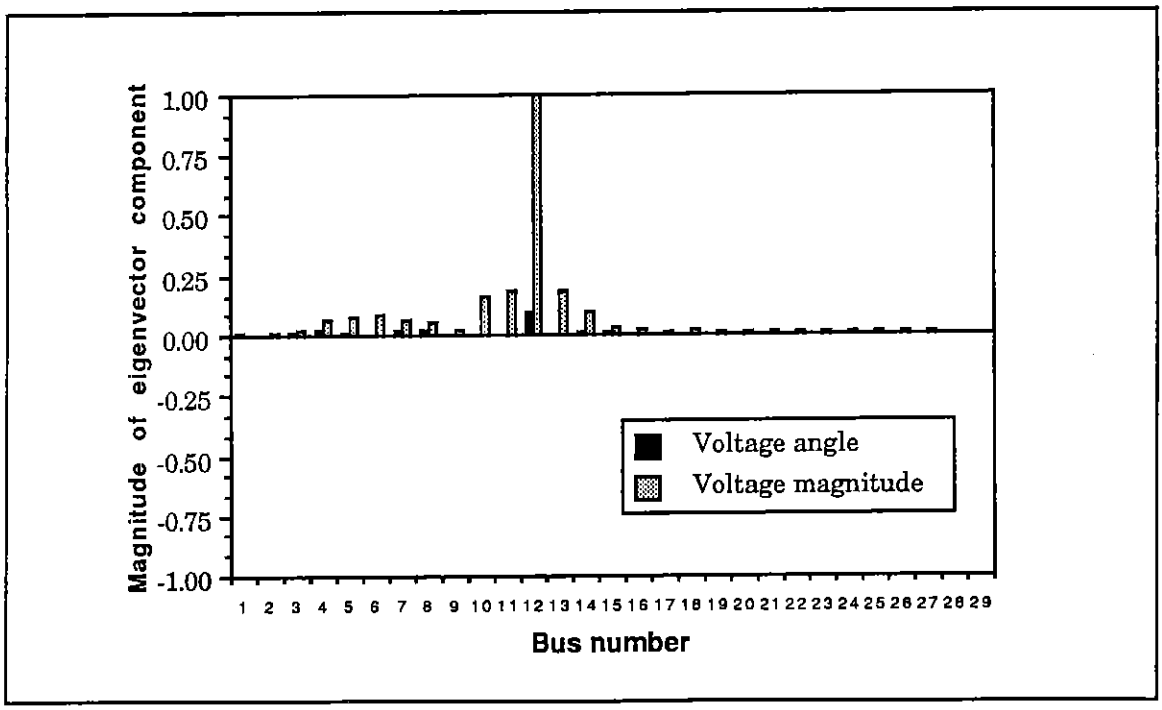

Figure 3-3 : Components of eigenvector associated with positive eigenvalue of UEP solution Jacobian when reactive load at bus 11 = 400 MVAR

This interpretation of the simplified method solutions suggests two methods of decreasing the number of buses which must be checked. First, in order to accurately model the interconnected electrical system, most utilities must include in their models (both planning and on-line) a large portion of the system (sometimes exceeding 50 percent of the total buses) which they do not own, operate, or have detailed real-time information. Therefore it is not necessary that the voltage vulnerability, and hence the corresponding simplified solutions, of these areas of the system be calculated. Second, vulnerability to voltage collapse is usually greatest in those portions of the system which have large loads and are electrically distant from voltage support. These areas can normally be rapidly determined through simple heuristic algorithms. These buses could then be checked first with the simplified method. Additionally, simplified solutions do not usually exist for those buses which do not contain load (such as those in the high voltage transmission system).

Using these two methods the number of buses which must be checked is initially decreased from n to n^*. The most straightforward way to calculate the pertinent solutions would be to perform Newton-Raphson powerflows using in turn each of the n^* initial voltage guesses. For the subset of low voltage solutions which exist, n^u, an energy measure could then be calculated for each, and the corresponding voltage vulnerability of the areas ranked.

However due to the nature of the low voltage solutions this would not be the most computationally efficient approach. The simplified method starts from the solved high voltage solution, and then only changes the voltage at a single bus i. This means that the nonzero mismatches initially occur only at bus i and its first neighbors, and that the elements of the high voltage Jacobian which must be initially changed are also only those associated with bus i and its first neighbors. Sparse vector methods [36] could then be used to perform the first iteration very efficiently. The computational order of updating the factored Jacobian (assumed to be available from the high voltage solution) is then proportional to the union of the factorization paths of i and its first neighbors. The length of these paths is normally quite small, even in large systems. The voltage correction vector $\Delta \mathbf{x}$ can then calculated using a fast forward and full back substitution. An initial approximation of the energy measure for a low initial guess at bus i is then $\vartheta^i(\mathbf{x}-\Delta\mathbf{x})$. These values could be ranked, with only those with an initial energy below a given threshold processed in more detail.

Experience has shown the deviation of the low voltage solution from the high voltage solution is normally localized about the bus with the original simplified method low voltage guess. This means that even if the entire system is solved for with a Newton-Raphson powerflow, the mismatches at most buses will be close to zero throughout the entire iterative process. The magnitude of energy difference provides a measure of the distance between the two solutions. Those solutions of most interest (characterized by a small energy differences) also tend to be the most localized solutions. This property can be exploited through techniques such as the zero mismatch (ZM) approach proposed in [37]. In the ZM approach rather than computing mismatches and voltage correction for the entire system, these operations are restricted to buses that have significant mismatches. Determining this subset of buses is not, however, always straightforward. For the first iteration it would just be bus i and its first neighbors. In subsequent iterations the subset of buses could be limited to those whose incident transmission lines experienced large changes in real or reactive power.

3.3 Optimal Multiplier Method

A new method of finding a low voltage solution for a system was recently presented in [38]. This technique exploits the convergence characteristics of the Newton-Raphson method when the powerflow equations are expressed in rectangular form (3-1). In order to explain this technique, it is necessary to first discuss the optimal multiplier theory originally presented in [35].

The powerflow equations in rectangular form (3-1) can be expressed as a set of quadratic equations having no first order terms:

$$\begin{bmatrix} s \end{bmatrix} = \theta(\mathbf{x}) = \begin{bmatrix} \mathbf{A} \end{bmatrix} \begin{bmatrix} x_1x_1 \\ x_1x_2 \\ \cdot \\ \cdot \\ x_ix_j \\ \cdot \\ \cdot \\ x_nx_n \end{bmatrix} \tag{3-4}$$

where A is a constant matrix of the susceptances and conductances from (3-1), $\mathbf{s} \in R^{2n}$ is the vector of the bus real and reactive power injections, and $\mathbf{x} \in R^{2n}$ is the vector of bus voltages expressed in rectangular coordinates. For any guess of $\mathbf{x}^k$, using a Taylor series expansion about $\theta(\mathbf{x}^k)$, the value of s can be expressed exactly (since A is constant) as

$$\mathbf{s} = \theta(\mathbf{x}^k) + \mathbf{J}(\mathbf{x}^k)\,\Delta\mathbf{x} + \theta(\Delta\mathbf{x}) \tag{3-5}$$

The standard method of solving using the Newton-Raphson powerflow is then to ignore the third term and obtain an approximation of $\Delta\mathbf{x}$ as

$$\Delta\mathbf{x} = \mathbf{J}(\mathbf{x}^k)^{-1}\,(\mathbf{s} - \theta(\mathbf{x}^k)) \tag{3-6}$$

The best direction to move to minimize the norm of the mismatch is then given by $\Delta\mathbf{x}$. The new voltage guess is then determined by

$$\mathbf{x}^{k+1} = \mathbf{x}^k - \mu\,\Delta\mathbf{x}$$

where μ is normally unity. However because (3-5) is exact, it is possible to solve directly for the value of μ which minimizes the norm of the mismatches in the direction $\Delta\mathbf{x}$. This analytic expression for μ is derived by first defining a cost function as

$$h = \|\mathbf{a} - \mu\mathbf{a} + \mu^2\mathbf{c}\|^2 \tag{3-7}$$

with

$$\mathbf{a} = \mathbf{s} - \theta(\mathbf{x}^k) = -\mathbf{J}(\mathbf{x}^k)\Delta\mathbf{x}$$
$$\mathbf{c} = -\theta(\Delta\mathbf{x})$$

Then solve for

$$\frac{\partial h}{\partial \mu} = g_3\mu^3 + g_2\mu^2 + g_1\mu + g_0 = 0 \tag{3-8}$$

where

$$g_0 = -\,\mathbf{a}\cdot\mathbf{a}$$

$$g_1 = \mathbf{a}\bullet\mathbf{a} + 2\,\mathbf{a}\bullet\mathbf{c}$$
$$g_2 = -3\,\mathbf{a}\bullet\mathbf{c}$$
$$g_3 = 2\,\mathbf{c}\bullet\mathbf{c}$$

Since (3-8) is a cubic equation, it has three roots. The roots are either three real numbers, or one real and two imaginary numbers. For the latter case, (3-7) only has a single local minimum value in the direction of $\Delta\mathbf{x}$. The value is a minimum because unless $\mathbf{a}$ and $\mathbf{c}$ are zero (which means we are at the solution), (3-7) goes to infinity as μ goes to $\pm\infty$. For the case of three real roots, there will be two local minima of (3-7) and a single local maximum in the direction of $\Delta\mathbf{x}$. Define μ as the smallest (or only) real root of (3-7), and μ_2 and μ_3 as either the imaginary roots or as the middle and largest real roots.

In [38] an interesting convergence property of the Newton-Raphson powerflow method using rectangular coordinates is reported. When a pair of multiple solutions of the powerflow equations are located close to each other, the powerflow tends to converge in the direction of the line containing the two solutions. If the convergent loci are exactly on this line, it is then possible to calculate the two solutions directly using the optimal multiplier, since each solution is a global minimum of (3-7) (note that even though the solutions are distinct, each is still a global minimum since the value of (3-7) is equal to zero at each solution). The authors provide no mathematical explanation as to why the method works, but rather provide a number of test results supporting their hypothesis.

However it is possible to prove that once an iterant $\mathbf{x}^k$ is an element of the line passing through two solutions, all subsequent elements of the iteration sequence $\{\mathbf{x}^l\}$, $l \geq k$, will also be elements of this line. Define $\mathbf{x}^s$ and $\mathbf{x}^u$ as two distinct solutions of the powerflow equations (3-1), with $\mathbf{x}^s$ being the stable high voltage solution, and $\mathbf{x}^u$ the unstable low voltage solution . The line through $\mathbf{x}^s$ and $\mathbf{x}^u$ is defined as the set

$$\mathbf{L} = \{\, \mathbf{x} \mid \mathbf{x} = (1-\lambda)\mathbf{x}^s + \lambda\mathbf{x}^u\,,\ \lambda \in R\}$$

Let

$$\mathbf{x}^s = \mathbf{x}^k + \mathbf{B}$$
$$\mathbf{x}^u = \mathbf{x}^k - \alpha\mathbf{B}$$

where $\mathbf{x}^k$ and $\mathbf{B}$ are vectors of the same dimension of $\mathbf{x}$, $\mathbf{x}^k \in \mathbf{L}$, $\mathbf{x}^k \neq \mathbf{x}^s$, $\mathbf{x}^k \neq \mathbf{x}^u$, and $\alpha \in R$.

Then since (3-5) is an exact Taylor expansion and (3-4) is a set of quadratic equations with no first order terms, we can write,

$$\mathbf{s} = \theta(\mathbf{x}^k) + \mathbf{J}(\mathbf{x}^k)\mathbf{B} + \theta(\mathbf{B})$$
$$\mathbf{s} = \theta(\mathbf{x}^k) - \alpha\mathbf{J}(\mathbf{x}^k)\mathbf{B} + \alpha^2\theta(\mathbf{B})$$

Assuming that $\mathbf{J}(\mathbf{x}^k)$ is nonsingular, the new direction $\Delta\mathbf{x}$ from the Newton-Raphson powerflow is given by (3-6). We must then show that $\Delta\mathbf{x}$ is tangent to $\mathbf{L}$ or equivalently that $\Delta\mathbf{x} = \lambda\mathbf{B}$ where $\lambda \in R$. Since from (3-6)

$$\Delta\mathbf{x} = \mathbf{J}(\mathbf{x}^k)^{-1}\,(\mathbf{s} - \theta(\mathbf{x}^k) = \mathbf{B} + \mathbf{J}(\mathbf{x}^k)^{-1}\theta(\mathbf{B})$$

we can write

$$\Delta\mathbf{x} = \mathbf{B} + \mathbf{J}(\mathbf{x}^k)^{-1}\theta(\mathbf{B}) \;=\; -\alpha\mathbf{B} + \alpha^2\mathbf{J}(\mathbf{x}^k)^{-1}\theta(\mathbf{B})$$

Solving for $\mathbf{J}(\mathbf{x}^k)^{-1}\theta(\mathbf{B})$ in terms of $\mathbf{B}$ we get

$$\mathbf{J}(\mathbf{x}^k)^{-1}\theta(\mathbf{B}) = \frac{1+\alpha}{\alpha^2-1}\mathbf{B}$$

Provided $\alpha \neq 1$ we can write $\Delta\mathbf{x}$ as a linear function of $\mathbf{B}$

$$\Delta\mathbf{x} \;=\; \mathbf{B} + \frac{1+\alpha}{1-\alpha^2}\mathbf{B} \;=\; \frac{2+\alpha-\alpha^2}{1-\alpha^2}\mathbf{B}.$$

Because $\Delta\mathbf{x}$ is tangent to L, the new point $\mathbf{x}^{k+1} = \mathbf{x}^k + \Delta\mathbf{x}$ is also an element of $\mathbf{L}$. ♦

As an example of the optimal multiplier method, consider the three bus system from Figure 2-10. For a load of 150 MWs at both buses 1 and 2, the system has the two solutions shown in Table 3-1.

Table 3-1 - Three Bus System Solutions

Bus Number	High Solution		Low Solution	
	e	f	e	f
1	0.7979	-0.1665	0.5203	-0.1778
2	0.7347	-0.2127	0.1909	-0.1887
3	1.0	0.0	1.0	0.0

To calculate both solutions, the standard Newton-Raphson algorithm is first performed, with the optimal multipliers being calculated each iteration. The first five columns of Table 3-2 shows these values, along with the maximum mismatch, for each iteration. To illustrate that the solution is actually converging along the line through $\mathbf{x}^s$ and $\mathbf{x}^u$, the last column in Table 3-2 shows the angle (in degrees) between the vector from $\mathbf{x}^u$ to $\mathbf{x}^s$ and the vector from $\mathbf{x}^s$ to $\mathbf{x}^k$. Since the angle is converging to zero, $\mathbf{x}^k$ is also converging towards the line through $\mathbf{x}^s$ and $\mathbf{x}^u$.

Table 3-2 - Newton-Raphson Iterations for Three Bus System

Iteration	Mismatch	μ	μ_2	μ_3	Angle
0	150.00	1.036	1.347 ±1.4j	41.3	
1	43.78	1.153	4.581	6.741	8.4°
2	5.82	1.027	20.42	36.05	5.7°
3	0.16	1.001	684.7	1321.0	3.3°
4	1.2e-6	1.000	9.22e5	1.23e6	1.7°

For those iterations in which three real optimal multipliers are obtained, the cost function h (3-7) has two local minimums in the direction $\Delta\mathbf{x}$. These local minimums occur at $\mathbf{x}^k - \mu_1\Delta\mathbf{x}$ (normally the high voltage solution) and $\mathbf{x}^k - \mu_3\Delta\mathbf{x}$ (normally the low voltage solution). The value of the cost function $h(\mathbf{x}^1 - \lambda\Delta\mathbf{x})$ (after the first iteration from Table 3-2) is plotted in Figure 3-4 as a function λ. As would be expected, the local minima occur at $\lambda = 1.1$ (μ) and 6.7 (μ_3). Since the angle between the solutions is not yet close to zero, the value of $h((\mathbf{x}^1 - \mu_3\Delta\mathbf{x})$ is rather high. However as the angle between the solutions goes to zero, the value of the $h((\mathbf{x}^k - \mu_3\Delta\mathbf{x})$ also tends towards zero.

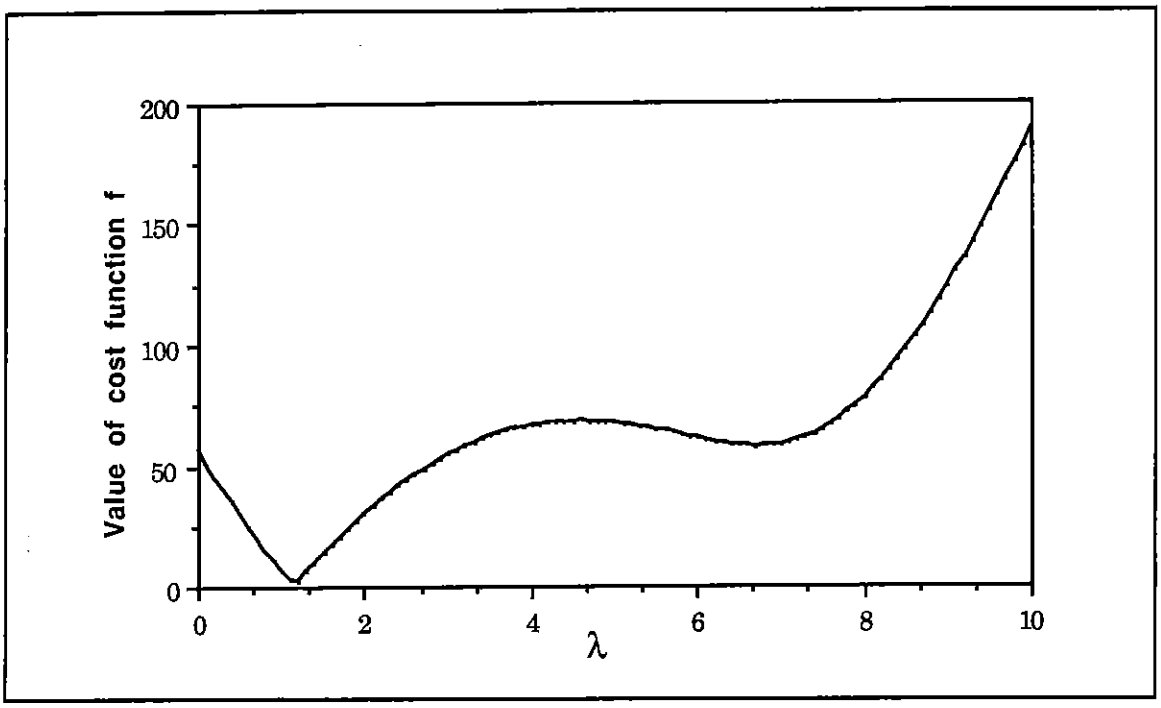

Figure 3-4: Variation of Cost Function in Direction $\Delta \mathbf{x}$

Once the high voltage solution has been solved with sufficient accuracy, a guess of the low voltage solution is then given by

$$\mathbf{x}^{u0} = \mathbf{x} - \mu_3 \Delta \mathbf{x} \tag{3-9}$$

The error associated with this estimate is a function of how close the angle between the solution vectors is to zero. The value of the low voltage solution can then be computed precisely using the standard Newton-Raphson algorithm with $\mathbf{x}^{u0}$ as the initial guess.

Since the cost of calculating the optimal multipliers is negligible compared to the cost of the rest of the Newton-Raphson algorithm, the optimal multiplier method provides a quick method of determining an initial guess of a low voltage solution. The accuracy of the value from (3-9) appears to be a function of how close the relative closeness of the two solutions. When the three bus load at bus 1 and 2 was 190 MWs (close to the critical load of 192 MWs), the value of $h(\mathbf{x}^{u0})$ was just 0.001 MVA. However as the load was decreased (causing the solutions to move apart), the value of $h(\mathbf{x}^{u0})$ increased, reaching 6.6 MVA for a load of 150 MW and 37 MVA when the load was 100 MW.

The optimal multiplier method can be used on arbitrary sized systems. However a problem develops when a generator's reactive output is saturated at one solution (the generator is modeled as PQ) while still regulating at the other solution (PV). Because of the type switching of the generator from PV to PQ (or vice versa), the matrix A from (3-4) is no longer identical for both solutions. Therefore the two solutions are no longer both defined as minima of (3-7). Nevertheless, this perturbation is not too severe, $\mathbf{x}^{u0}$ can often still provide a fairly good starting guess to locate the low voltage solution.

3.4 Energy Contour Search Method

An alternative technique to determining the closest UEP is to expand the constant contours of the energy function ϑ until the first point $\mathbf{x}^u$ satisfying $\theta(\mathbf{x}^u) = 0$ (where θ corresponds to the real and reactive powerflow mismatch equations defined in [3-1]) is encountered. This is equivalent to a minimizing the norm of the powerflow mismatch equations, subject to the constraint that energy is equal a given value.

Starting from the stable operating point, where $\vartheta = 0 = c^0$, the value of the target energy contour would be defined as $c^1 = c^0 + \Delta c$, where Δc would be a problem dependent (possibly user specified) value. Then the following minimization would be performed:

$$\min \{ \mathbf{h}(\mathbf{x}) \text{ such that } \vartheta(\mathbf{x}) = c^1 \}$$

where

$$h(\mathbf{x}) = \frac{1}{2}\theta(\mathbf{x})^T\theta(\mathbf{x}) = \frac{1}{2}\| \theta(\mathbf{x}) \|_2^2$$

Following the minimization, the value of $h(\mathbf{x})$ would be compared to a tolerance. If $h(\mathbf{x})$ is less than the tolerance, then a low voltage solution (hopefully the closest) has been found. Otherwise, the value of c is again incremented, $c^{i+1} = c^i + \Delta c$, and the process is repeated.

The actual minimization is performed using the iterative generalized reduced gradient method. At each loop k within the iteration the following three steps are performed. First, the vector $\mathbf{x} \in R^{2n}$ is partitioned into the dependent and independent variables y and $\mathbf{z}$ respectively, where y is a scalar. Let the values of y and $\mathbf{z}$ be given by

$$y = [x_r]$$

$$z = [x_1, x_2, \ldots, x_{r-1}, x_{r+1}, \ldots, x_{2n}]$$

Next, the equation $\vartheta(y^{k+1},z^k) = c^i$ is solved treating y^{k+1} as an unknown, and z^k as fixed. This is a simple one dimensional nonlinear problem. This problem can often be solved quite rapidly using an iterative procedure in which $\vartheta(y^{k+1},z^k)$ is approximated using a second order Taylor expansion

$$\vartheta(y^{k+1},z^k) = c^i \approx \vartheta(y^k,z^k) + \frac{\partial\vartheta(y^k,z^k)}{\partial y}\Delta y + \frac{1}{2}\frac{\vartheta^2(y^k,z^k)}{\partial y^2}(\Delta y)^2 \qquad (3\text{-}10)$$

The value of Δy can then be determined by the quadratic equation (if [3-10] has no real solution, then $\mathbf{x}$ must be repartitioned with a different variable chosen for y). Then $y^{k+1} = y^k + \Delta y$. Since the Taylor expansion is not exact, an iterative approach is needed. However experience has shown that seldom more than one or two iterations are needed. The calculation of $\partial\vartheta/\partial y$ is straightforward since $\nabla\vartheta(\mathbf{x})$ is just the powerflow mismatch equations neglecting transfer conductances, with the reactive mismatch j scaled by V_j^{-1}. The calculation of $\partial^2\vartheta/\partial y^2$ is correspondingly similar to the calculation of a diagonal element of the powerflow Jacobian and is computationally dependent only upon the first neighbors of y.

Once the value of y^{k+1} is determined and hence a point on the contour $\vartheta(\mathbf{x}) = c^i$ located, the reduced gradient direction is given by

$$\Delta z = -\left(\frac{\partial h}{\partial z} - \frac{\partial h}{\partial y}\left[\frac{\partial\vartheta}{\partial y}\right]^{-1}\frac{\partial\vartheta}{\partial z}\right) \qquad (3\text{-}11)$$

where

$$\frac{\partial h}{\partial z} = \theta^T(\mathbf{x})\,\mathbf{J}_z(\mathbf{x})$$

$$\mathbf{J}_z(\mathbf{x}) = \frac{\partial\theta}{\partial z} = \text{ the powerflow Jacobian, without the column corresponding to y.}$$

Then $\mathbf{z}^{k+1} = \mathbf{z}^k + \mu\Delta\mathbf{z}$ where μ is a scalar "step-size" parameter. Ordinarily the value of μ which minimizes h(**x**) would have to be determined using a line search method such as the Fibonacci or golden section techniques. However because of the structure of h(y,z+$\mu\Delta$z), it is possible to determine μ analytically using the optimal multiplier method from the previous section (3-7). However because the direction of movement, $\Delta\mathbf{z}$, is no longer defined by (3-6), (3-7) has to be rewritten as

$$h = \| \mathbf{a} + \mu\mathbf{b} + \mu^2\mathbf{c} \|^2 \qquad (3\text{-}12)$$

with

$$\mathbf{a} = \mathbf{s} - \theta(\mathbf{x}^k)$$
$$\mathbf{b} = \mathbf{J}_z(\mathbf{x})\Delta\mathbf{z}$$
$$\mathbf{c} = -\theta(\Delta\mathbf{x})$$

The coefficients of (3-8) are then redefined as

$$g_0 = \mathbf{a}\bullet\mathbf{b}$$
$$g_1 = \mathbf{b}\bullet\mathbf{b} + 2\,\mathbf{a}\bullet\mathbf{c}$$
$$g_2 = 3\,\mathbf{b}\bullet\mathbf{c}$$
$$g_3 = 2\,\mathbf{c}\bullet\mathbf{c}$$

As before, the roots of the cubic equation are used to determine the minimum(s) of (3-12) in the direction $\Delta\mathbf{z}$.

Consider the application of the energy contour search method to the two bus system from Figure 2-1. Figure 3-5 shows the contours of the energy function in the e_2-f_2 space and is therefore just a mapping of Figure 2-3 from the V_2-α_2 space into the e_2-f_2 space (although the values of the contours plotted were changed). Since there are only two unknowns, e_2 and f_2, both y and z are scalars. Let $y = e_2$ and $z = f_2$. For convenience in illustrating the method, Δc is chosen to be 0.43, which is one half the energy of the unstable equilibrium point.

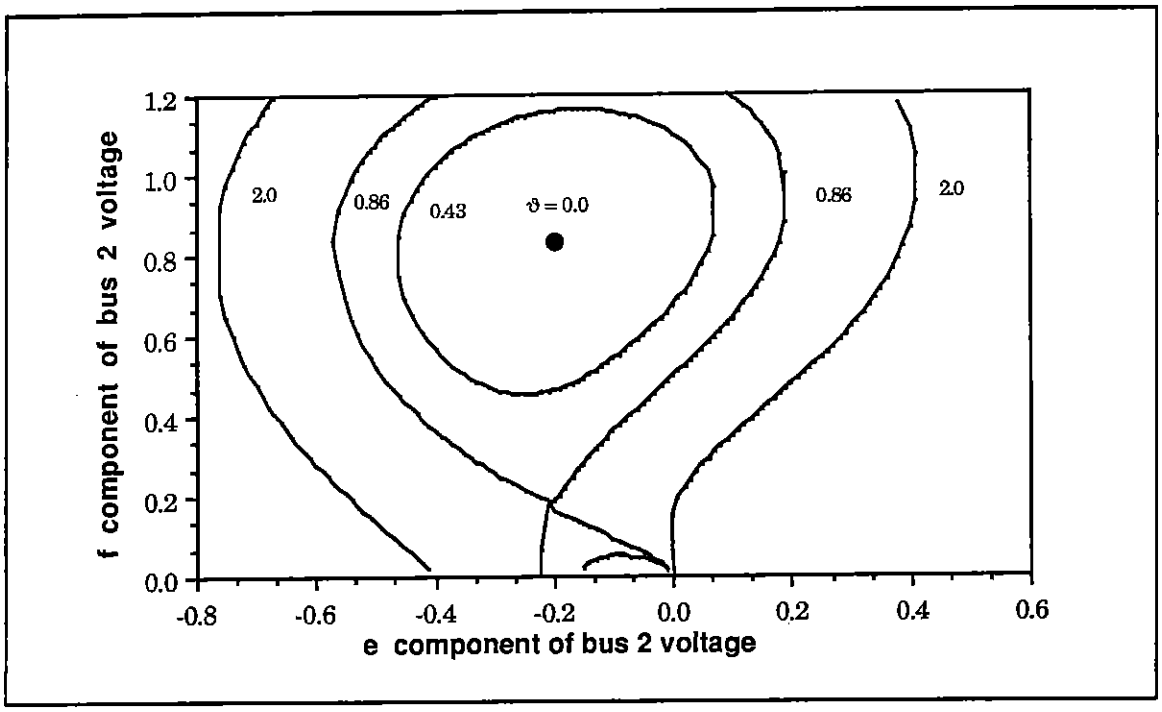

Figure 3-5 : Energy Function Contours in e_2-f_2 Plane

The value of y^1 is calculated using equation (3-10) iteratively. Figure 3-6 compares the value of ϑ as a function of y with the quadratic approximation of (3-10) for the first iteration. After the first iteration, the value of $\vartheta(y^1,z^0)$ was 0.368, while after the second iteration it was 0.4298. Since |0.43 - 0.4298| was below the convergence tolerance, the next step was the calculation of Δz using (3-11). Then the cost function was minimized in the direction Δz. The upper half of Table 3-3 shows the values of y (e_2) and z (f_2) after each iteration, along with the values of the cost function and energy difference after both the y and z portions of each iteration. After three iterations the algorithm had converged close enough to the minimum of h(x) subject to the constraint that $\vartheta(x) = 0.43$. The value of c^2 was then set to 0.86 and the process repeated. The lower half of Table 3-3 shows the results of these iterations.

Table 3-3 Energy Contour Iterations for 2 Bus System

Iteration	y (e_2)	z (f_2)	Cost y	Cost z	ϑ_y	ϑ_z
desired energy contour = 0.43						
0	0.831	-0.200	0.000		0.00	
1	0.462	-0.243	0.598	0.493	0.43	0.41
2	0.452	-0.243	0.485	0.485	0.43	0.43
3	0.452	-0.243	0.485	0.485	0.43	0.43
desired energy contour = 0.86						
0	0.452	-0.243	0.485		0.43	
1	0.201	-0.207	0.092	0.018	0.86	0.85
2	0.174	-0.201	0.003	0.001	0.86	0.86
3	0.169	-0.200	0.000	0.000	0.86	0.86

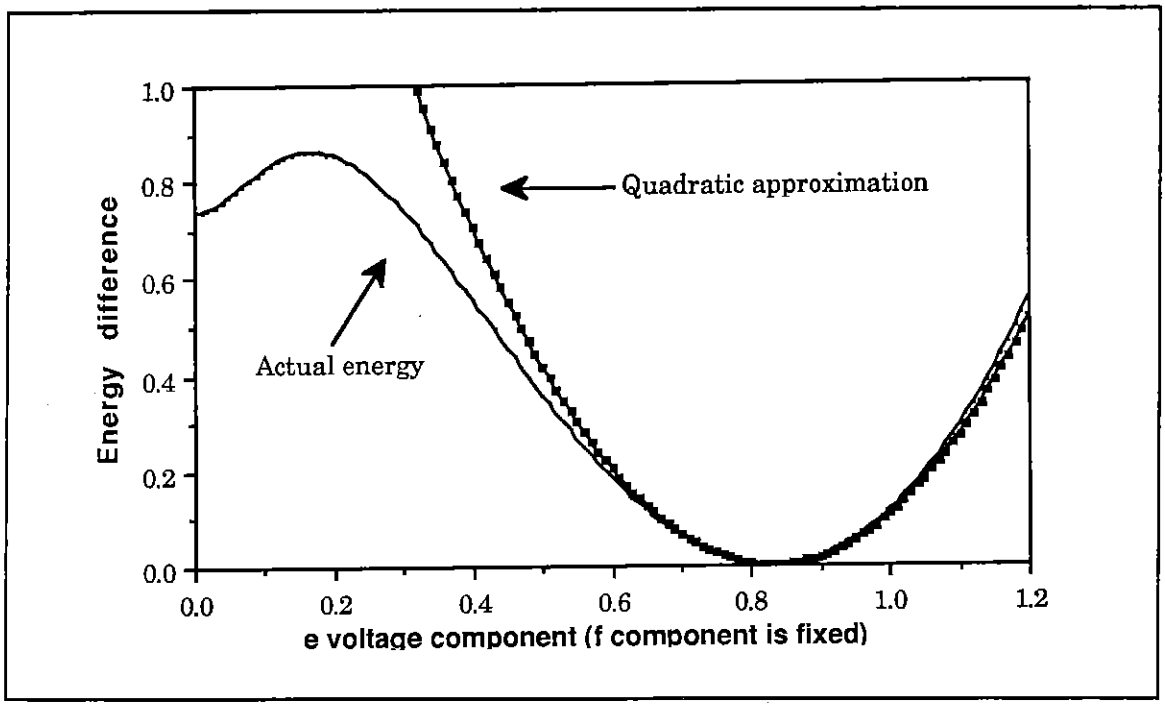

Figure 3-6 : Energy Function and Quadratic Approximation

The energy contour method provides an alternative to the earlier methods, which are dependent upon the convergence characteristics of the Newton-Raphson powerflow. The advantage of this method is that if the minimum of the cost function can be found for each contour, the method would provide a straightforward way of determining the most pertinent low voltage solutions, namely those with the lowest energy differences.

However the application of the energy contour method does present at least two challenges. First, it is possible that the constraint set $\vartheta = c$ may contain a number of local minimums of the cost function. An example of such an occurrence is shown in Figure 2-18 for a loading of approximately 520 MVARs at bus 11. There are two low voltage solutions which have identical energy values of approximately 7.30. The problem in using the constant contour method is determining whether a given minimum is actually the global minimum. If the value is not the global minimum, it is possible that a low voltage solution with the same energy has been missed. Testing on larger systems seems to indicate that the (local) minimum which is found depends upon the initial choice of the dependent variable y. This is not unsurprising since the initial direction of movement is dictated by the choice of the dependent variable. Second, the computational requirements of the method, and its success in locating the closest low voltage solution, is dependent upon the energy contour stepsize Δc chosen. In the preceding example where the energy value was known beforehand, Δc was chosen for convenience to simply be one-half the energy value. However in an actual problem the choice of Δc is much more difficult. If Δc is too small the computational cost of the method could become excessive. However if Δc is too large it is possible that the method could skip over low voltage solutions.

Chapter 4 - Conclusions and Proposals

This report has discussed the application of an energy based method for assessing the vulnerability of electrical power systems to voltage collapse. Proximity of a power system to voltage collapse is determined from the energy difference between the stable operating point and one or more unstable equilibrium points. This energy difference provides smoothly varying measure of proximity to voltage instability which could be used to determine when a power system is in danger of voltage collapse. The computational cost of the method appears to be tractable.

There are, however, a number of directions for further research before the method is mature enough for implementation in a utility control center. First, a computationally efficient algorithm needs to be developed for locating the pertinent low voltage solutions of the system. A number of possible solutions to this problem were presented in Chapter 3. Further testing of the improvements to the Simplified Method presented in 3.2.2 needs to be performed. The method needs to implemented on a larger system to determine the computational costs involved and to examine modifications for optimal performance. The Optimal Multiplier method in section 3.3 also offers promise of being able to rapidly determine the closest low voltage solution. Key questions which need to be researched include how close two solutions must be before the method works and how the method could be altered to handle limits on system controllers. The Energy Contour Search method from section 3.4 also offers opportunity for further research. The severity of the problem of the nonuniqueness of the energy contour cost function minima needs to be determined, with possible refinements to the algorithm to alleviate this problem examined. Also a method needs to be determined to choose appropriate values of the energy contour stepsize Δc. .

The second major area of future research concerns modifications to the system models and energy function to include more detailed system devices and dynamics. In particular the effects of high voltage DC (HVDC) lines, generator excitation systems, and time delays in on-load tap changing transformers need to be researched. HVDC lines, which are used to transport large amounts of power over long distances, can have a substantial impact upon the voltage behavior in the surrounding AC systems. Additionally their fast-acting control systems offer potential to mitigate some system voltage instability problems. Research is needed to determine how the system model and energy function should be modified to accommodate HVDC lines. A second possible area for expansion of the system model is a

more detailed representation of generator excitation systems. Excitation systems are used to regulate the generator voltage. The voltage stability of an electrical system is dependent not only upon the electromechanical models, but also upon the effects of the generator excitation systems. However, whether the effects of these systems need to be modeled in greater detail for the time frame of the voltage instability problems considered in this report needs to be determined. Another system device which merits further research is the on-line tap changing transformer. The ability of transformers to change their tap ratios to regulate voltages has already been included in the system models. However there are often time delays on the order of a few minutes before these controllers respond to voltage changes. Since this delay is close to the time frame of the voltage collapse problem, their effect on system stability needs to be investigated.

Third, more research is needed into the modeling of power systems at the low voltage solutions. As was mentioned earlier, a number of effects such as controller limits have already been included in the model. Whether the models need to be expanded to include additional effects of operating at voltages substantially below their normal operating ranges needs to be determined. For example the load models used in the examples throughout the report have assumed that load is independent of bus voltage. While valid for some load types over the time period of the study, more detailed load models will probably have to include voltage dependence.

Finally, the energy method should be demonstrated on systems larger than the 30 bus example used here. The application of the method to larger systems will motivate computational improvements in calculating the appropriate low voltage solutions.

The work to date on the application of an energy based security method to the problem of voltage instability in power systems appears successful. However significant theoretical and computational questions remain before the method is mature enough for actual implementation in a utility control center.

References

[1] C. Barbier and J-P Barret, "Analysis of Phenomena of Voltage Collapse on a Transmission System," *Revue Generale de l'electricite*, Vol. 89, October 1980, pp. 672-680.

[2] A. Kurita and T. Sakurai, "The Power System Failure on July 23, 1987 in Tokyo," *Proc. 27th IEEE Conf. on Decision and Control*, Austin, TX, Dec. 1988.

[3] North American Electric Reliability Council, *1987 System Disturbances*, pp. 18, July 1988.

[4] C.W. Taylor, "Voltage Stability Analysis with Emphasis on Load Characteristics and Undervoltage Load Shedding," Panel paper, IEEE PES Summer Meeting, Long Beach, Ca, July 1989.

[5] T.J. Bertram, K.D. Demaree and L.C. Dangelmaier, "An Integrated Package for Real-Time Security Enhancement," *PICA Proc.*, pp. 18-25, Seattle, WA, May 1989.

[6] M. Chau et. al., "Understanding Voltage Collapse in Bulk Transmission Systems," *Engineering Foundation Conference on Bulk Power System Voltage Phenomena: Voltage Stability and Security,*" Potosi, MO, Sep. 1988.

[7] B.M. Weedy and B.R. Cox, "Voltage Stability of Radial Power Links," *Proc. IEE*, vol. 115, no. 4, pp. 528-536, April 1968.

[8] G. A. Cucchi, "Voltage Stability and Security, the Operator's View: 'Seeing More Now but Enjoying it Less'," *Engineering Foundation Conference on Bulk Power System Voltage Phenomena: Voltage Stability and Security,*" Potosi, MO, Sep. 1988.

[9] C.W. Brice et. al., "Physically Based Stochastic Models of Power System Loads," U.S. Dept. of Energy Report DOE/ET/29129, Sept. 1982.

[10] D.I. Sun et al., "Optimal Power Flow by Newton Approach," *IEEE Transactions on Power App. and Sys.*, vol. PAS-103, pp. 2864-2880, Oct. 1984.

[11] F.L. Alvarado and T.H. Jung, "Direct Detection of Voltage Collapse Conditions," *Engineering Foundation Conference on Bulk Power System Voltage Phenomena: Voltage Stability and Security,*" Potosi, MO, Sep. 1988.

[12] C. Lemaitre et al., "An Indicator of the Risk of Voltage Profile Instability for Real-time Control Applications," IEEE PES Summer Meeting, SM 713-9, Long Beach, CA, July 1989.

[13] Y. Sekine, A. Yokoyama and Y. Kumano, "A Method for Detecting a Critical State of Voltage Collapse," *Engineering Foundation Conference on Bulk Power System Voltage Phenomena: Voltage Stability and Security,*" Potosi, MO, Sep. 1988.

[14] A. Tiranuchit and R.J. Thomas, "A Posturing Strategy Against Voltage Instabilities in Electrical Power Systems," *IEEE Trans. on Power Systems*, vol. PWRS-3, pp. 87-93, Feb. 1988.

[15] A. Tiranuchit et al., " Towards a Computationally Feasible On-line Voltage Instability Index," *IEEE Trans. on Power Systems*, vol. PWRS-3, pp. 669-675, May 1988.

[16] P. Kessel and H. Glavitsch, "Estimating the Voltage Stability of a Power System," *IEEE Trans. on Power Systems*, vol. PWRS-1, pp. 346-354, July 1986.

[17] R.A. Schlueter et al., "Reactive Supply; On-line Security Criteria," *Engineering Foundation Conference on Bulk Power System Voltage Phenomena: Voltage Stability and Security,*" Potosi, MO, Sep. 1988.

[18] A. Yokoyama and Y. Sekine, "A Static Voltage Stability Index based on Multiple Load Flow Solutions," *Engineering Foundation Conference on Bulk Power System Voltage Phenomena: Voltage Stability and Security,*" Potosi, MO, Sep. 1988.

[19] M. Vidyasagar, *Nonlinear Systems Analysis*, Prentice-Hall, Englewood Cliffs, NJ, 1978.

[20] M.A. Pai and P.W. Sauer, "Stability Analysis of Power Systems by Lyapunov's Direct Method," *IEEE Control Magazine*, Jan. 1989.

[21] A.R. Bergen and D.J. Hill, "A Structure Preserving Model for Power Systems Stability Analysis, " *IEEE Trans. Power App. and Sys.*, vol. PAS-101, pp. 25-35, Jan. 1981.

[22] C.L. DeMarco and A.R. Bergen, "Application of Singular Perturbation Techniques to Power system Transient Analysis," I.S.C.A.S. Proc., pp. 597-601, Montreal, May 1984 (abridged version); also Electronics Research Laboratory, Memo. No. UCB/ERL M84/7, U. of CA, Berkeley (complete version).

[23] C.L. DeMarco, "A New Method of Constructing Lyapunov Functions for Power Systems," IEEE International Symposium on Circuits and Systems, Espoo, Finland, June 1988.

[24] Y. Tamura, K. Iba and S. Iwamoto, "A Method of Finding Multiple Load Flow Solutions for General Power Systems", *IEEE PES Winter Meeting*, A 80 043-0, New York, Feb. 1980.

[25] H. Chiang, "Study of the Existence of Energy Functions for Power Systems with Losses," *IEEE Trans. Circuits and Systems*, pp. 1423-1429, Vol. CAS-36, no. 11, Nov. 1989.

[26] H. Chiang and J.S. Thorp, "The Closest Unstable Equilibrium Point Method for Power System Dynamic Security Assessment," *IEEE Trans. Circuits and Systems*, pp. 1187-1200, Vol. CAS-36, no. 9, Sep. 1989.

[27] C.L. DeMarco and A.R. Bergen, "A Security Measure for Random Load Disturbances in Nonlinear Power System Models," *IEEE Trans. Circuits and Systems*, pp. 1546-1557, vol. CAS-34, no. 12, Dec. 1987.

[28] T.J. Overbye and C.L. DeMarco, "Voltage Security Enhancement Using Energy Based Sensitivities," Accepted at IEEE PES Winter Meeting, Atlanta, GA, Feb. 1990.

[29] A. Klos and A. Kerner, "The Non-Uniqueness of Load-Flow Solutions," *Proc. PSCC V.*, 3.1/8, 1975.

[30] Y. Tamura et al., "Monitoring and Control Strategies of Voltage Stability based on Voltage Instability Index," *Engineering Foundation Conference on Bulk Power System Voltage Phenomena: Voltage Stability and Security*," Potosi, MO, Sep. 1988.

[31] I. Dobson and H. Chiang, "Towards a Theory of Voltage Collapse in Electric Power Systems," *Systems & Control Letters*, pp. 253-262, 1989.

[32] C.B. Garcia and W.I. Zangwill, *Pathways to Solutions, Fixed Points and Equilibria*, Englewood Cliffs, NJ, Prentice-Hall, 1983.

[33] R.A. Schlueter et al., "Voltage Stability and Security Assessment," EPRI Report El-5967, Project 1999-8, August, 1988.

[34] Y. Tamura, K. Sakamoto, Y. Tayama, "Voltage Instability Proximity Index (VIPI) based on Multiple Load Flow Solutions in Ill-Conditioned Power Systems," Proc. 27 IEEE Conf. Decision and Control, Austin, TX, Dec. 1988.

[35] S. Iwamoto and Y. Tamura, "A Load Flow Calculation for Ill-conditioned Power Systems," *IEEE Trans. Power App. and Sys.*, vol PAS-100, pp. 1736-1743, April 1981.

[36] W.F. Tinney, V. Brandwajn and S.M. Chan, "Sparse Vector Methods", *IEEE Trans. Power App. and Sys.*, vol PAS-104, pp. 295-301, Feb. 1985.

[37] R. Bacher and W.F. Tinney, "Faster Local Power Flow Solutions: The Zero Mismatch Approach," *IEEE Trans. on Power Systems*, vol. PWRS-4, pp. 1345-1354, Nov. 1989.

[38] K. Iba et al., "A Method for Finding a Pair of Multiple Load Flow Solutions in Bulk Power Systems," *PICA Proc.*, pp. 98-104, Seattle, WA, May 1989.

[39] J. Vegte, *Feedback Control Systems* , Prentice-Hall , Englewood Cliffs, NJ, 1986.